

Evaporation of light particles from a hot, deformed and rotating nucleus *

K. Pomorski

*Department of Theoretical Physics, M. Curie-Skłodowska University
ul. Radziszewskiego 10, 20-031 Lublin, Poland*

J. Bartel, J. Richert

*Laboratoire de Physique Théorique, Université Louis Pasteur,
3, rue de l'Université, 67084 Strasbourg Cedex , France*

and

Centre de Recherches Nucléaires, BP 28, F-67037 Strasbourg Cédex 2

K. Dietrich

*Physik Department, Technische Universität München,
James Franck Straße, D-85747 Garching, F.R.G.*

Abstract

The dependence of the transmission coefficient on the deformation, the collective rotation and excitation energy of the compound nucleus emitting light particles is introduced in the framework of Weißkopf's evaporation theory. The competition between fission and particle evaporation is treated by a Langevin equation for the fission variable coupled to the emission process. Detailed calculations are presented on the decay of different Gd and Yb isotopes at an excitation energy of about 250 MeV. These calculations demonstrate the importance of the effects of nuclear deformation and of the initial spin distribution on the evaporation.

*Partially supported by the Polish State Committee for Scientific Research under contract No. 2 P302 052 06

1 Introduction

The properties of excited nuclei in thermal equilibrium are of great physical interest. We are interested in excitation energies below some (400–500) MeV, where we may still describe the nucleus as a system of neutrons and protons which interact by effective forces. All the information on the physical state of hot nuclei is then to be obtained from a careful study of their decay by emission of neutrons, protons, and α -particles and their decay by fission. The emission of photons will be neglected, as we consider energies far above the thresholds for particle emission.

The basis of our approach [1] is a description of the particle emission as a purely statistical process, as given by the Weißkopf theory [2], and the nuclear fission as a transport process [3]. The importance of the non-statistical aspects of the fission process in this context was recognized by Grangé and Weidenmüller [4]. Our approach and also the ones of Fröbrich, Abe and Carjan [5, 6, 7] are based on the premises of their work.

Our efforts are dedicated to a stepwise improvement of this general theory in order to reach a quantitatively reliable description of the decay of the compound nuclei.

In the present paper, we give a more careful study of how the evaporation probabilities depend on the deformation of the nucleus, on its excitation and on its collection rotation. In the standard form of the evaporation theory [2], the deformation of the decaying nucleus enters only through the level densities of the initial and final nucleus. We take into account that the transmission coefficient also depends on the deformation and, to a smaller degree, on the collective rotation of the nucleus. This will be explained in Chapter 2.

Our research is encouraged by the increasing amount of careful experimental studies of the evaporation of light particles from excited nuclei and of the concomitant decay by fission [8]. The results of our calculations are presented and compared with experimental work, especially of that of Ref. [9] in Chapter 3.

Finally, we summarize in Chapter 4 our findings and point out the direction of our future work.

2 Description of Fission Dynamics Including Evaporation

The fission process of hot and rotating nuclei should be described within a statistical model which takes into account the effect of energy dissipation due to the coupling to the internal degrees of freedom modelled by a friction force which generates diffusion. The corresponding transport equation of the Fokker-Planck (FPE) type was originally proposed for nuclear fission by Kramers in Ref. [3] and later on adapted for heavy ions physics in Ref. [10] - [12]. It is not easy to solve this equation exactly when the number of collective coordinates and conjugate momenta is larger than 2. An effective but

approximate method of solving the FPE based on the moment expansion was used in [11]. Unfortunately the probability distributions in the multidimensional space of collective coordinates is usually far from a gaussian form and the moment expansion method fails [13]. It is important to recall here that the set of differential equations which one obtains in the moment expansion method for the average coordinates and momenta is simply the set of classical equations of motion with friction as e.g. those used by Blocki and co-workers [14]. A more efficient way of solving the transport equations based on Monte Carlo method has been proposed in Ref. [15]. It was also shown in [1] that the Monte Carlo calculation combined with the local moment expansion method transforms the FPE into a set of equations of motion containing random forces which is equivalent to a set of coupled Langevin equations. The Langevin equation has already been used in [16] in order to describe heavy-ion collisions and fission [17]. This idea is very fruitful and allows us to describe many phenomena occurring in heavy-ion physics and fission due to statistical fluctuations (see e.g. the review article [5]).

In Chapter 2 we will present the physical basis of our model and explain how we couple the emission of light particles to the dynamical evolution of the system from the compound nucleus state to the scission point. This dynamics is governed in our description by the Langevin equation which we will present in Sect. 2.1, before explaining in Sect. 2.2 how particle emission is incorporated into this description. In Sect. 2.3 and 2.4 we deal with the initial conditions and the integration of the Langevin equation.

2.1 Equations of Motion

We need to describe the time evolution of the nuclear system from an initial state which corresponds to a compound-nucleus at high excitation and angular velocity but usually created close to spherical symmetry to a final state in which a large amount of excitation and angular momentum will have been dissipated. For such a description we use a single collective coordinate $q = \rho_{cm}/R_0$ which measures the distance between the centers of mass of the two halves of the fissioning nucleus in units of the radius R_0 of the corresponding spherical nucleus. For the time being we restrict our description to symmetric fission. The description of asymmetric fission would necessitate the introduction of an additional collective coordinate describing the mass asymmetry of the two emerging fission fragments. If p designates the conjugate momentum associated with the collective coordinate q we obtain the following equations of motion describing the time evolution of the fissioning nucleus:

$$\frac{d q}{d t} = \frac{p}{M(q)} , \quad (1)$$

$$\frac{d p}{d t} = \frac{1}{2} \left(\frac{p}{M(q)} \right)^2 \frac{d M}{d q} - \frac{d V}{d q} - \frac{\gamma(q)}{M(q)} p + F_L(t) . \quad (2)$$

In these equations $M(q)$ represents the collective mass, $V(q)$ the potential and $\gamma(q)$ the friction coefficient [21]. The potential V is calculated as the difference between the Helmholtz free energies of the deformed and spherical nucleus. The friction coefficient

γ is calculated in the framework of the *wall* and *window* friction model [18, 19]. The explicit expressions of these quantities, as obtained in the framework of the Trentalange-Koonin-Sierk shape parametrization [20], have been presented and discussed in detail in Ref. [21]. The quantity $F_L(t)$ designates the random Langevin force which couples the collective dynamics to the intrinsic degrees of freedom. This Langevin force is chosen to be a gaussian random variable with zero mean value. In practice eqs. (1) - (2) are discretized by introducing a sufficiently small time step τ . Then the equations take the form

$$q(t + \tau) - q(t) \approx \frac{p}{M(q)} \tau \quad (3)$$

$$p(t + \tau) - p(t) \approx \frac{1}{2} \left(\frac{p}{M(q)} \right)^2 \frac{dM}{dq} \tau - \frac{dV}{dq} \tau - \frac{\gamma(q)}{M(q)} p \tau + \sqrt{D(q)} f_L(\tau) . \quad (4)$$

Here $f_L(\tau) = \sqrt{\tau} \eta$ where η is a gaussian distributed random number with $\langle \eta \rangle = 0$ and $\langle \eta^2 \rangle = 2$ and where the brackets represent ensemble averages. The diffusion coefficient $D(q)$ appearing in eq. (4) is related to the friction coefficient $\gamma(q)$ through the Einstein relation

$$D(q) = \gamma(q) T . \quad (5)$$

This relation holds in linear response theory as a high-temperature approximation of the dissipation-fluctuation theorem. In the applications presented below the nuclear temperature will always be sufficiently high so that eq. (5) is approximately verified. To speak at all about a nuclear temperature already supposes that the excitation of the nuclear system is shared to equal parts by all of the nucleonic degrees of freedom, so that statistical models apply. To simplify the description we consider the excited nucleus in a statistical description as member of a **grand-canonical ensemble** which can be characterized by a temperature T . For such a description to make sense, we need to assume that the time scale which governs the fission dynamics is sufficiently long compared to the one which determines the internal equilibration of the nuclear excitation among all the nucleons. If this is the case, we can assume that the system can be considered as being continuously at equilibrium. In this framework the temperature T is simply a measure of the nuclear excitation energy E^* and related to the latter through the usual Fermi gas relation $E^* = a(q) T^2$ where $a(q)$ is the level density parameter of the considered nucleus at a nuclear deformation characterized by q . The excitation energy itself is determined by the conservation of the total energy as will be discussed in section 2.4 below.

2.2 Particle Emission

The process of light particle emission from a compound nucleus is governed by the emission rate Γ_ν^α at which a particle of type ν (neutrons, protons and α particles are considered here) is emitted at an energy in the range $[e_\alpha - \frac{\Delta e_\alpha}{2}, e_\alpha + \frac{\Delta e_\alpha}{2}]$ before the compound nucleus eventually undergoes fission.

Several theoretical approaches have been proposed in order to describe the emission from a deformed, highly excited and rotating nucleus [1, 5, 7]. The method which we present below is close in spirit to the one used in [1], but in our description the widths Γ_ν^α for particle emission will in addition depend on the deformation and angular momentum of the compound nucleus [22].

According to Weisskopf's conventional evaporation theory [2] the partial decay rate $\Gamma_\nu^{\alpha\beta}(E^*, L)$ for emission of a light particle of type ν with energy e_α and orbital angular momentum ℓ_β from a compound nucleus with excitation energy E^* rotating with an angular momentum L can be written as

$$\Gamma_\nu^{\alpha\beta}(E^*, L) = \frac{2S_\nu + 1}{2\pi\hbar\rho(E^*, L)} \sum_{L_R=|L-\ell_\beta|}^{L+\ell_\beta} \int_{e_\alpha-\Delta e_\alpha/2}^{e_\alpha+\Delta e_\alpha/2} w_\nu(e, \ell_\beta; \chi) \rho_R(E_R^*, L_R) de, \quad (6)$$

where

$$\rho(E^*, L) = (2L + 1) \left(\frac{\hbar^2}{2\mathcal{J}} \right)^{3/2} \sqrt{a} \frac{e^{2\sqrt{a}E^*}}{12E^{*2}} \quad (7)$$

is the level density in the emitting nucleus. The level density ρ_R in the residual (daughter) nucleus with the excitation energy E_R and the angular momentum L_R is obtained in the same way. Both these quantities also depend on the mass and charge number and on the nuclear deformation. The quantities \mathcal{J} and a represent the moment of inertia and the level density parameter of the compound nucleus and S_ν the intrinsic spin of the emitted particle. $w_\nu(e, \ell; \chi)$ is the transmission coefficient for emitting a particle of type ν , with energy e and angular momentum ℓ from the deformed compound nucleus. The parameter χ in the argument list of w_ν stands for all quantities not explicitly mentioned here, such as the mass and charge number, the nuclear deformation, the direction in space in which the particle ν is emitted. Proceeding in this way would, however, leads to hardly tractable numerical problems, since in the Langevin formalism which we endeavour here, we need to follow the dynamics of the fissioning nucleus plus evaporation for a very large number of trajectories (of the order of 10^6). We therefore use a simplified procedure which introduces a transmission coefficient $\bar{w}_\nu(e, \ell; \chi)$ obtained by a double averaging over the different emission directions and over the whole surface of the deformed compound nucleus. A detailed description of how $\bar{w}_\nu(e, \ell; \chi)$ is calculated in the framework of the Hill-Wheeler approximation [23] and how the averaging procedure is carried out is given in Appendix A. With this averaged transmission coefficient \bar{w} the width Γ_ν^α for emission of a particle of type ν and energy e_α reads:

$$\Gamma_\nu^\alpha(E^*, L) = \frac{2S_\nu + 1}{2\pi\hbar\tilde{\rho}(E^*)} \int_{e_\alpha-\Delta e_\alpha/2}^{e_\alpha+\Delta e_\alpha/2} w_\nu^{eff}(e; \chi) \tilde{\rho}_R(E_R^*) de, \quad (8)$$

where

$$\tilde{\rho}(E^*) = \frac{\rho(E^*, L)}{2L + 1}$$

is the angular momentum independent part of the density (7) and a similar relation holds for $\tilde{\rho}_R$. The effective transmission coefficient in (8) is obtained by performing a summation over all allowed angular momenta of the emitted particle and those of the daughter nucleus:

$$w_\nu^{eff}(e; \chi) = \frac{1}{2L+1} \sum_{\ell_\beta=0}^{\ell_{max}} \sum_{L_R=|L-\ell_\beta|}^{L+\ell_\beta} (2L_R+1) \bar{w}_\nu(e, \ell_\beta; \chi) \quad , \quad (9)$$

here ℓ_{max} is the maximal angular momentum available for the particle having the energy e . As already mentioned the emission width Γ_ν^α also depends on the mass and charge number A and Z as well as on the deformation of the compound nucleus.

Once the emission widths Γ_ν^α known, one can establish the emission algorithm which decides at each time step $[t, t+\tau]$ along each of the trajectories if a particle is emitted from the compound nucleus. It is the value of the emission width Γ_ν^α which ultimately have to decide which of the light particles is emitted and at which energy. Since Γ_ν^α represents the rate at which a particle of type ν and energy e_α is emitted, the total emission rate for a particle of given type, irrespectively of the energy at which it is emitted, is given by

$$\Gamma_\nu(E^*, L) = \frac{2S_\nu + 1}{2\pi\hbar\tilde{\rho}(E^*)} \int_0^{e_{max}} w_\nu^{eff}(e; \chi) \tilde{\rho}_R(E_R^*) de = \sum_{\alpha=1}^n \Gamma_\nu^\alpha(E^*, L) \quad , \quad (10)$$

where we have replaced the upper integration limit by some large enough constant e_{max} (which will, a priori, be different for the different particles) and at which the probabilities for particle emission will essentially have vanished. n is the number of energy bins of width Δe_α in the interval $[0, e_{max}]$. The emission rate Γ for emission of any kind of particles is the sum of the Γ_ν :

$$\Gamma = \Gamma_n + \Gamma_p + \Gamma_\alpha \quad . \quad (11)$$

First of all we need to decide whether a particle is emitted at all in the given time interval $[t, t + \tau]$. The probability for emitting any particle is given, for a small enough time step τ , by

$$P(\tau) = 1 - e^{-\Gamma\tau} \approx \Gamma\tau \quad . \quad (12)$$

One then draws a random number η_1 in the interval $[0, 1]$. If $\eta_1 < P(\tau)$ a light particle is emitted. If the time step τ is chosen sufficiently small, the probability for emitting a particle will be small. In this way we guarantee that in a time interval at most one particle is emitted and we avoid to consider the emission of more than one particle in each time interval.

In the case that a particle is emitted one needs to decide next of which type this particle is. To this purpose one draws a second random number η_2 in the interval $[0, 1]$ and determines the localisation of η_2 with respect to the covering of this interval by the three bins Γ_n/Γ , Γ_p/Γ , and Γ_α/Γ . Depending on the bin in which η_2 is located, a neutron, or a proton or an α particle is emitted.

We still have to determine the energy with which this particle is emitted, and we accomplish this in the following way. We introduce the quantity

$$\Pi_\nu(e_\alpha) = \frac{1}{\Gamma_\nu} \left\{ \frac{2S_\nu + 1}{2\pi\hbar\tilde{\rho}(E^*)} \int_0^{e_\alpha} w_\nu^{eff}(e; \chi) \tilde{\rho}_R(E_R^*) de \right\}, \quad (13)$$

which represents the probability that a particle of type ν is emitted with an energy smaller than e_α . The quantity covers the interval $[0, 1]$. Subdividing the interval $[0, 1]$ in a certain number of equal bins, one decides with which energy the light particle is emitted by drawing a third random number η_3 in the interval $[0, 1]$. Inverting the function in eq. (13) $\Pi_\nu^{-1}(\eta_3)$ will fall in one energy bin

$$\Pi_\nu^{-1}(\eta_3) \in [e_\alpha - \frac{\Delta e_\alpha}{2}, e_\alpha + \frac{\Delta e_\alpha}{2}] \quad (14)$$

of the total interval $[0, e_{max}]$ and thus decide on the energy with which the particle is emitted.

2.3 Initial Conditions

The description of the fission process including particle emission starts, in principle, from an initial state corresponding to a spherical or deformed compound nucleus whose shape is characterized by the collective coordinate q_0 , the corresponding conjugate initial momentum p_0 , the excitation energy E_0^* (with corresponding temperature $T_0 = \sqrt{E_0^*/a(q_0)}$) and the initial total angular momentum L_0 . In practice the excitation energy E^* may be known approximately from the experiment. This is, however, not the case for q_0 , p_0 and the angular momentum L_0 . In the calculations presented and discussed in Sect. 4 we choose q_0 corresponding to a spherical nucleus and draw the conjugate momentum p_0 for each trajectory from a normalized gaussian distribution

$$P(p_0) = \frac{1}{\sqrt{2\pi m T_0}} \exp[-\frac{p_0^2}{2m T_0}]. \quad (15)$$

Here m is the collective inertia at the deformation q_0 . It is in principle experimentally possible to determine the distribution of initial angular momenta for instance by measuring the γ multiplicities [24]. As these distributions are rarely available, we chose L_0 to have a fixed value but we shall discuss below the dependence of the final results on the choice of L_0 .

2.4 Integration of the Langevin Equation

Once the initial conditions are fixed one can integrate the system of equations of motion (1-2) using their finite difference version (3-4). At each time step $[t, t + \tau]$ one draws a random number η from a gaussian distribution which defines the fluctuating force in eq.

(4) and thus generates a trajectory in the variable q . Simultaneously one asks, as just explained, whether a light particle is emitted and decides, eventually, of its type ν and energy e_α .

At the beginning of the whole process the system has a fixed total energy E_{tot} which is the sum of the collective kinetic and potential energy

$$E_{coll} = \frac{p^2}{2M(q)} + V(q)$$

and a collective rotation energy

$$E_{rot} = \frac{L^2}{2\mathcal{J}}$$

corresponding to a rigid deformed rotator of moment of inertia \mathcal{J} [25, 26]. The excitation energy E^* at time $(t + \tau)$ and thereby the temperature of the nucleus is redetermined at each time step through the conservation of the total energy

$$E_{tot} = E_{coll}^{(i)} + E_{rot}^{(i)} + E_i^* = E_{coll}^{(f)} + E_{rot}^{(f)} + E_f^* + e_\alpha + B_\nu + E_{recoil} \quad , \quad (16)$$

where the indices i or f refer to the initial (time t) or final state (time $t + \tau$). B_ν is the binding energy of the emitted particle (which is zero unless an α particle is emitted), e_α is its kinetic energy after emission and E_{recoil} is the recoil energy of the nucleus due to the emission process. These three quantities enter the equation only when a light particle is emitted in the time interval $[t, t + \tau]$. Since the recoil energy is in any case very small, it will be neglected. Additionally it is assumed that the deformation as well as the angular frequency of the nucleus is not changed due to the particle emission.

It is evident that each emission of a light particle carries away excitation energy and angular momentum and thereby increases the height of the fission barrier of the residual nucleus which, in turn, renders the fission event less and less probable.

For each choice of the initial conditions one generates in this way a separate trajectory which is followed through in time. Emitted particles and their energies are registered. Each trajectory can either lead to fission if it overcomes the fission barrier and continues on to the scission point, or can end up as a rather cold compound nucleus if too much energy has been lost to make the crossing of the fission barrier possible. Sampling the total number of trajectories N_{fiss} which have led to fission defines the fission cross section as $\sigma_{fiss} = N_{fiss}/N$ with N equal to the total number of trajectories.

Let us finally mention that it is important to take into account the fact that the α is a composite particle and that its emission therefore presupposes its existence in the nucleus prior to emission. This is in principle quantified by the introduction of a preformation factor whose value can in principle be determined [27]. Since this quantity is, however, very poorly known, we fix it in the following by multiplying the emission width Γ_α by a factor f_α ($0 \leq f_\alpha \leq 1$). The choice of f_α will be discussed in the following.

3 Results

We study the decay of compound nuclei of several isotopes of $_{64}\text{Gd}$ and of $_{70}\text{Yb}$ at various excitation energies ranging from 150 MeV to 300 MeV. We selected these nuclei because a careful experimental investigation of their decays is available [7] and because they are known to exhibit large ground state deformations. Consequently, it is of special interest to investigate the influence of deformation on the emission of n , p and α particles from excited states of these nuclei.

The results concern the following physical aspects:

- i The dependence of the emission probabilities of neutron, protons, and α -particles on the deformation, the excitation energy and the angular momentum of the emitting nucleus (Figs. 1 to 9).
- ii The dependence of the emission probabilities $\Pi_\nu(e)$, eq. (13), of a particle of given type ν on the kinetic energy e (Figs. 10 to 15).
- iii The dependence, at different temperatures T , of the number of fission events and light-particle multiplicities on the time t (Figs. 16 to 18). Although these functions are not measurable, they are important for the physical understanding of the decay, especially the transient time phenomenon [4] and its dependence on the temperature.
- iv The spectral distribution of the emitted particles (Figs. 19 to 21).
- v The dependence of the multiplicities, fission cross section and barriers on the initial angular momentum of the nucleus (Figs. 22 to 25).
- vi The influence of the friction forces on the multiplicities of the emitted particles (Fig. 26).

We will now give a detailed description of these points.

3.1 Dependence of the emission probabilities on the nuclear deformation

In Figs. 1–3, the emission width Γ_ν , eq. (10), for n , p , and α -particles is shown as a function of the deformation ρ_{cm}/R_0 of the emitting source. The initial ensemble of decaying nuclei consists of $_{70}^{160}\text{Yb}_{90}$ nuclei at an excitation energies of 50 MeV, 150 MeV and 250 MeV respectively, and with a rotational angular momentum $L = 40\hbar$. All the emission rates are seen to grow as a function of increasing deformation. This trend can be easily understood as for increasing deformation the transmission occurs through a larger surface. This effect has already been observed for all three particles [28]. We notice, however, that the emission width for α -particles increases more steeply than the one for n and p for the two lower excitation energies $E^* = 50$ MeV (Fig. 1) and $E^* = 150$ MeV (Fig. 2). This is due to the fact that, as the nucleus is elongated, the barrier

height for charged particles is reduced in the section of the surface which is farther away from the nuclear center and increased in the section which are closer to the center. The section where the barrier is diminished is larger than the section where it is increased. Consequently, the emission rate for charged particles increases faster than the one for neutrons.

In Figs. 4, 5, and 6 the deformation dependences of the emission rates for n , p , and α particles are shown for different values of the rotational angular momentum, varying between $L = 0\hbar$ and $60\hbar$. For n and p the influence of the rotation on the emission rate is seen to be negligible, whereas the emission rate of α particles grows by 10%–20% as the rotational angular momentum increases from $0\hbar$ to $60\hbar$. It is clear that the centrifugal force, which helps to overcome the barrier, is largest for the α -particle. Furthermore, the centrifugal effects matter the more the larger the barrier. The barrier for the α -particle is larger than the one for n and p .

Let us point out that the rotational angular momentum of the nucleus has a very noticeable influence on the height of the fission barrier which decreases as a function of increasing angular momentum. Thus, at high angular momentum, nuclear fission can compete more effectively with evaporation.

In Figs. 7–9, the deformation dependent emission width for n , p and α is shown for two different isotopes of both ${}_{64}\text{Gd}$ and ${}_{70}\text{Yb}$. The results can be easily understood: for given proton number, the emission width Γ_n for neutrons is the larger the larger the neutron number (see Fig. 7). On the other hand, for given neutron number, the emission width Γ_p for protons is the larger the larger the proton number (see Fig. 8). At given proton number, the emission width Γ_α , for α -particles decreases with increasing neutron surplus whereas, at given neutron number, Γ_α grows with increasing proton number (see Fig. 9). This is a simple consequence of the fact that the α -particle contains an equal number of neutrons and protons.

3.2 Behaviour of the probability $\Pi_\nu(e)$

An interesting quantity is the probability $\Pi_\nu(e)$ to emit a particle of type ν with an energy smaller than e . Its definition in terms of the emission rate $\Gamma_\nu(e)$ is given in eq. (13). The emission width Γ_ν depends also on the shape of the emitting nucleus, and so does the integrated probability $\Pi_\nu(e)$.

In Figs. 10 to 12, the probability $\Pi_\nu(e)$ is shown for the emission of neutrons, protons, and α -particles. In each of the figures, $\Pi_\nu(e)$ is plotted separately for the case that the emitting nucleus has a spherical shape, the shape corresponding to the saddle and the scission point. In all cases the fissioning nucleus is ${}^{160}\text{Yb}$ at an initial excitation energy $E^* = 250\text{ MeV}$ and an initial angular momentum $L = 40\hbar$. All curves show a monotonous increase of Π_ν as a function of the energy e starting from a minimal energy e which is zero for neutrons, but finite for protons and α -particles due to the acceleration of the charged particles in the Coulomb field of the residual nucleus. For neutron emission, the dependence of $\Pi_n(e)$ on the deformation of the emitting nucleus is very small, whereas for protons and α -particles the curves $\Pi_\nu(e)$ are shifted to somewhat higher energies for the

spherical source. The physical interpretation is that the Coulomb barrier is larger for the spherical nucleus than for the deformed nucleus and consequently the threshold for proton or α -emission is at a higher energy than for neutrons. We note that the scission shape for a nucleus like ^{160}Yb consists essentially of two tangent, slightly deformed fragments of half the charge.

In Figs. 13 to 15 the probability $\Pi_\nu(e)$ is shown for neutrons, protons, and α -particle emission for 3 different excitation energies of the initial compound nucleus $^{160}_{70}\text{Yb}$. The shape of the emitting nucleus is chosen here as corresponding to the saddle point and its initial angular momentum is fixed at $L = 40 \hbar$. It is seen that the rise of the probability Π_ν as a function of e is the steeper the smaller the excitation energy. Such a behaviour can be easily understood since the range of energies of the emitted particles must rise with excitation energy. We have also investigated the dependence of the functions $\Pi_\nu(e)$ on the neutron and proton numbers of the initial ensemble of compound nuclei, comparing the emission from the 4 nuclei $^{144}_{64}\text{Gd}$, $^{154}_{64}\text{Gd}$, $^{150}_{70}\text{Yb}$, and $^{160}_{70}\text{Yb}$, in each case for the same excitation energy (150 MeV), the same angular momentum ($40 \hbar$) and the same shape (saddle point). The results are indistinguishable for the emission of neutrons and only very slightly dependent on the nature of the emitting nucleus for the emission of protons and α -particles.

3.3 Time dependence of the multiplicities and the number of fission events

The dependence of the number of decays of a given type on the time which elapses starting with the formation of the compound nucleus is unfortunately not measurable. Nevertheless, we think that it is interesting to exhibit this dependence for a few cases since it enables us to gain insight into the dynamical mechanism.

In Fig. 16 we show the number of fission events as a function of the time t on a logarithmic scale. This result was obtained with the light-particle evaporation channels turned off. The initial compound nucleus is $^{160}_{70}\text{Yb}$ with an initial angular momentum $L = 40 \hbar$. The 3 curves in Fig. 16 correspond to 3 different initial temperatures resulting in 3 different initial fission barrier heights U_B . It is seen that the transient time increases with decreasing excitation energy, as one expects. It should be noted that the functions $N_{\text{fiss}}(t)$ obtained for $T = 4$ MeV look quite similar to those for $T = 5$ MeV and are just shifted along the $\log(t)$ axis. Furthermore, if t_0 is the time where half of the final number $N_{\text{fiss}}(\infty)$ of fission events have occurred

$$N_{\text{fiss}}(t_0) = \frac{1}{2} N_{\text{fiss}}(\infty) \quad (17)$$

we may approximate N_{fiss} for times close to t_0 by a linear function of $\log(t)$

$$N_{\text{fiss}}(t) \approx N_{\text{fiss}}(t_0) + \kappa_0 \log \frac{t}{t_0} \quad (18)$$

As one infers from Fig. 16, the dependence on the initial temperature is mainly contained in the quantity t_0 whereas the factor κ_0 in (18) is almost the same for $T = 5$ MeV and

$T = 4$ MeV. The approximate time dependence (18) which is valid during part of the transient time interval is seen to be totally different from the one in the Kramers regime which is valid in the cases when the fission barrier is much higher than the temperature of the fissioning nucleus.

In Fig. 17 we show the multiplicity (number of emitted particles in coincidence with fission and per compound nucleus) for the emission of neutrons, protons and α -particles as a function of time for the decay of a compound nucleus ${}^{160}_{70}\text{Yb}$ at an initial excitation energy of 293 MeV and an initial angular momentum of $45 \hbar$. It is seen that the emission of p and α -particles ceases already after some $3 \cdot 10^{-21}$ sec whereas the number of emitted neutrons still increases. Again this is easily understood as a result of the different thresholds for charged and uncharged particles.

In Fig. 18 the fraction N_{fiss}/N of nuclei undergoing fission is shown for the initial compound nucleus ${}^{160}_{70}\text{Yb}$ as a function of time. Now, contrary to the results presented in Fig. 16, the emission of light particles is taken into account. The initial excitation energy of the nucleus is $E^* = 293$ MeV and the initial angular momentum $L = 45 \hbar$ is assumed. The well-known Kramers approximation holds whenever there is an approximately constant current across the fission barrier which implies a linear dependence of the number of fission events upon time. It is seen from the figure that there is in fact no clearly distinguished section with a linear time-dependence. At best one could replace the function by a straight line in the interval between 8 and $12 \cdot 10^{-21}$ sec. The “transient time”, i.e. the time needed for the build-up of an approximately constant fission current is seen to be $\sim 8 \cdot 10^{-21}$ sec. This is the main part of the time available for fission events. It is thus clear that the use of the Kramers approximation or of the still simpler statistical transition state hypothesis for the whole time interval would lead to wrong results.

Furthermore the very concept of a constant current across the fission barrier, which is the pre-requisite of the Kramers approximation could lose its validity because of the existence of light particle emission which implies that the excitation energy and the angular momentum changes for those compound nuclei which emit a light particle prior to fission.

3.4 Spectral distribution of the emitted particles

In Fig. 19, we present the probability per energy unit of neutron, proton, and α -particle emission as a function of the energy of the emitted particle. This figure is made on the basis of 10^6 trajectories. The solid curves show the spectral distribution in coincidence with fission, i.e. for particles emitted from nuclei which subsequently undergo fission. The dashed curves represent the spectral distribution in anti-coincidence with fission, i.e. for particles emitted from nuclei which subsequently end up as evaporation residues. The initial compound nucleus is ${}^{160}_{70}\text{Yb}$ at 293 MeV excitation energy and an angular momentum of $52 \hbar$. The curves for different types of emitted particles are displaced against each other because charged particles gain energy in the Coulomb field of the residual nucleus. Furthermore, the thresholds for emission of n , p , and α are in general different.

In addition, for α -particles, the spectral distribution for particles emitted in coincidence with fission is slightly shifted towards smaller energies as compared to the distribution obtained when measured in anti-coincidence with fission. This is probably due to the fact that charged particles are preferentially emitted from the pole tips around the long half axis. The larger deformation then implies a smaller gain of kinetic energy from the repulsive Coulomb field.

In Figs. 20 and 21, the normalized yield for neutron emission is shown as a function of the nuclear deformation in the fission and evaporation channels. The reader should notice that for nuclei which undergo fission, the emission of neutrons takes place, on the average, at a larger deformation than for the nuclei which end up as evaporation residues. This is due to the fact that the distribution of the fissioning nuclei moves towards the saddle point in the deformation landscape. This effect should give rise to an experimentally observed anisotropy in the angular distribution of prefission particles different from the one observed in the angular distribution of particles emitted by the evaporation residua. The distribution for the case when the emission of protons and alpha particles is inhibited is shown in Fig. 20 by the short-dashed line. It is seen that this distribution is very close to the one obtained when the emission of all three kinds of particles is allowed. The initial angular momentum is different for the two Figs. 20 and 21. It is seen that the maximum of the distribution of the neutrons emitted by the evaporation residua is shifted with increasing angular momentum towards larger deformations. The difference in the average deformation of the both distributions should be directly reflected in the difference in the anisotropy of the angular distributions of prefission neutrons and those emitted by the residua.

3.5 Dependence of the multiplicities on the initial angular momentum of the compound nucleus

The multiplicity of prefission neutrons, protons and alpha particles is plotted in Figs. 22–23 as a function of the initial angular momentum L . The initial compound nucleus is ^{160}Yb with the initial excitation energy $E^*=251$ MeV in Fig. 22 and 293 MeV in Fig. 23. The corresponding fission rates are plotted in Fig. 24. It is seen in Figs. 22 – 23 that the neutron multiplicity decreases significantly with growing L while that for protons and alphas is much less affected. This is due to the fact that for large angular momenta the fission barriers U_B become small (see Fig. 25) and it takes a shorter time to reach the scission configuration. Consequently less neutrons are emitted on the average when the barrier is small. Alpha particles and protons are mostly emitted in the initial stage when the excitation energy of the nucleus is large, so that their multiplicities depend more weakly on the initial L . The effective fission rate (including particle emission) changes by 2 orders of magnitude (see Fig. 24) when one increases the value of the initial angular momentum by $12\hbar$ units up to its maximal value which corresponds to $U_B=0$. Fig. 23 shows that this also holds true for the higher excitation energy of $E^* = 293$ MeV.

This result indicates that a more precise knowledge of the initial spin distribution in compound nuclei is necessary in order to compare to the experiment. One has to stress

here that large L values contribute most to the experimental value of the multiplicities as already seen in Fig. 24. It therefore is certainly not correct to describe the experiment with a theoretical calculation using only the average value of the initial spin. As the fission barrier heights decrease strongly with increasing angular momentum as seen in Fig. 25, the higher L components which would lead to fission will have to be mocked up by an overestimation of the role of the fluctuating forces.

Assuming an equal population of the initial angular momenta, which is, as just mentioned, not the best approximation, we have estimated the average of the n , p and α -multiplicities. The resulting values are compared in Table 1 with the experimental data taken from Ref. [9]. All parameters of the model are those given in Sec. 2.1 and in Ref. [21]. We only have to assume the preformation factor $f_\alpha = 0.2$ (see discussion in Sec. 2.4) in order to reproduce the experimental number of alpha particles. This goes into the right direction since our calculations show that α particle emission is strongly enhanced by rotation and deformation effects.

3.6 Influence of the friction forces on multiplicities of precession particles

The role of the friction forces in fission of high excited compound nuclei is widely known. It was shown already in Ref. [4] that the nuclear viscosity influence significantly the precession neutron multiplicities. This effect was discussed later in almost all papers dealing with the problem. It was even assumed that the neutron multiplicities could be an indirect measure of the nuclear friction (see e.g. Ref. [8]).

The dependence of n , p and α -multiplicities on the magnitude of the friction coefficient connected with the elongation of the nucleus is plotted in Fig. 26 for ^{160}Yb at $E^*=293$ MeV and $L=50\hbar$. The strength of the friction coefficient is varied in the interval (0.02, 2) in units of its value given by the wall formula [14]. The neutron multiplicity for small values of the friction coefficient is about 30% smaller than obtained with the wall friction. As the transient time increases as a function of the friction, the increase of the multiplicity of neutrons emitted prior to fission is easily understood. Again the effect upon the emission of p and α -particles is small, because these particles are emitted in a relatively short time interval after the formation of the compound nucleus which is in our case small compared to the transient time. One has to notice that the results for very weak friction depend significantly both on the width of the initial distribution of the momentum conjugate with the fission coordinate (eq. (15)) and on the initial angular momentum. For larger values of the friction strength, close to γ_{wall} , the influence of the initial distribution of the momentum p_0 on the neutron multiplicity is weak (see also the discussion in Ref. [1]).

4 Summary and discussion

Our results demonstrate the importance of nuclear deformation on the evaporation of light particles from strongly excited nuclei. This dependence on the deformation plays an important role also for the competition between fission and particle emission and might modify the limits which were determined for the nuclear friction force [1] from the experimental data [6] on evaporation and fission. The dependence of the evaporation width on the rotational angular momentum was found to be negligible for the emission of n and p and rather small for the emission of α -particles. Let us, however, remind that the fission probability depends very sensitively on the angular momentum, as we have already emphasized in Ref. [1]. Due to this strong dependence of the fission probability on the initial angular momentum, it becomes very important to get precise information on the angular momentum distribution of the initial ensemble of compound nuclei. The outcome of the competition between light particle emission and fission may depend strongly on the initial angular momenta. Consequently, we have to try to obtain theoretical information on the angular momenta of the initial nuclei by treating the fission process dynamically [29, 30].

Agreement between calculated and measured emission probabilities for α -particles can only be obtained, if an empirical preformation probability for α -particles of about 0.2 is assumed. One of the most important further improvements of the theory will be to evaluate this preformation factor within the temperature-dependent Thomas-Fermi approximation which underlies our theory [27].

Another aspect which we intend to investigate is the angular dependence of emitted light particles when the angular momenta of the initial compound nuclei are aligned or the nuclei are polarized. In these cases it is conceivable that the angular dependence of the emitted particles shows a more pronounced dependence on the rotational angular momentum than the integrated yields we calculate in the present paper. One might also hope that the angular distribution of emitted particles depends on the deformation of the source nuclei sufficiently sensitively so as to determine the deformation from such measurements. Of course, experimental data on the angular distribution of emitted neutrons, protons, and α -particles from aligned rotating deformed nuclei would be of great interest for these studies.

Acknowledgments

One of us (K.P.) acknowledges gratefully the support during a four week stay in Garching by the Technical University Munich and support by the IN2P3 during a one month stay at C.R.N. in Strasbourg. J. B., K. D., and J. R. are very grateful for the kind hospitality extended to them at the UMCS. K. D. acknowledges financial support from the BMFT and also from the DAAD for the travel funds to Lublin.

References

- [1] E. Strumberger, K. Dietrich and K. Pomorski, Nucl. Phys. **A529** (1991) 522
- [2] V. Weisskopf, Phys. Rev. **52** (1937) 295
- [3] H. Kramers, Physica **7** (1940) 284
- [4] P. Grangé, H.C. Pauli and H.A. Weidenmüller, Phys. Lett. **B88** (1979) 9; Z. Phys. **A296** (1980) 107
- [5] P. Fröbrich, Nucl. Phys. **A545** (1992) 87c
- [6] G.R. Tillack, R. Reif, A. Schülke, P. Fröbrich, H.J. Krappe and H.G. Reusch, Phys. Lett. **B296** (1992) 296
- [7] Y. Abe, N. Carjan, M. Ohta, T. Wada, Proc. IN2P3–RIKEN Symp. on Heavy–Ion Collisions, Obernai, 1990, France
- [8] D. Hilscher and H. Rossner, Ann. Phys. Fr. **17** (1992) 471
- [9] M. Gonin, L. Cooke, K. Hagel, Y. Lou, J.B. Natowitz, R.P. Schmitt, S. Shlomo, B. Srivastava, W. Turmel, H. Ustunomiya, R. Wada, G. Nardelli, G. Nebbia, G. Viesti, R. Zanon, B. Fornal, G. Prete, K. Niita, S. Hannuschke, P. Gonthier and B. Wilkins, Phys. Rev. **C42** (1990) 2125
- [10] H. Hofmann and P.J. Siemens, Nucl. Phys. **A257** (1976) 165, Nucl. Phys. **A275** (1977) 464
- [11] Ch. Ngô and H. Hofmann, Z. Phys. **A282** (1977) 83
- [12] W. Nörenberg, Phys. Lett. **B52** (1979) 289
- [13] H. Hofmann in "Deep-Inelastic and Fusion Reactions with Heavy Ions", Berlin, 1979, Lecture Notes in Physics **117**, Springer Verlag, p. 64
F. Scheuter and H. Hofmann, Nucl. Phys. **A394** (1983) 477
- [14] J. Błocki, H. Feldmeier and W.J. Swiatecki, Nucl.Phys. **A459** (1986) 145
- [15] G. Lamm and K. Schulten, J. Chem. Phys. **78** (1983) 2713
- [16] P. Fröbrich and S.Y. Xu, Nucl. Phys. **A477** (1988) 143
- [17] Y. Abe, C. Gregoire and H. Delagrangé, J. de Phys. **C4** (1986) 47
- [18] J. Błocki, J. Randrup, W.J. Swiatecki, C.W. Tsang, Ann. Phys. **105** (1977) 427
- [19] J. Błocki, Y. Boneh, J.R. Nix, J. Randrup, M. Robel, A.J. Sierk and W.J. Swiatecki, Ann. Phys. **113** (1978) 330

- [20] S. Trentalange, S.E. Koonin and A. Sierk, Phys. Rev. **C22** (1980) 1159
- [21] J. Bartel, K. Mahboub, J. Richert and K. Pomorski, Z. Phys. **A**, accepted for publication
- [22] K. Dietrich, K. Pomorski and J. Richert, Z. Phys. **A351** (1995) 397
- [23] D.L. Hill, J.A. Wheeler, Phys. Rev. **89** (1953) 1102
- [24] W. Kühn, A. Ruckelshausen, R.D. Fisher, G. Breibach, H.J. Hennrich, V. Metag, R. Novotny, R.V.F. Janssens, T.L. Khoo, D. Habs, D. Schwalm, B. Haas and R.S. Simon, Phys. Rev. Lett. **62** (1989) 1103
- [25] K. Bencheikh, P. Quentin, J. Bartel, Nucl. Phys. **A571** (1994) 518.
- [26] E. Chabanat, et al., Phys. Lett. **325B** (1994) 13.
- [27] K. Dietrich et al, in preparation.
- [28] M. Blann, Phys. Rev. **C21** (1980) 1770
- [29] W. Przystupa, K. Pomorski, Nucl. Phys. **A572** (1994) 153.
- [30] K. Pomorski, W. Przystupa, J. Richert, Acta Phys. Polon. **B25** (1994) 751.

Appendix: Evaluation of the transmission coefficients w_ν

The explicit calculation of the transmission rates Γ_ν^α given by eq. (8) requires the knowledge of the average transmission coefficient $\bar{w}_\nu(e, \ell; \chi)$ for the emission of light particles from the nucleus into the continuum. In principle, a rigorous treatment would require the knowledge of $w_\nu(e, \ell; \chi)$ which appears in eq. (6) and should be calculated by averaging the transmission coefficients corresponding to the transmission of a particle emitted in a given direction from each point of the surface of the deformed, excited and rotating nucleus. This can be done in principle but is hardly possible in practice where these calculations must be carried out at each time step and over a very large ensemble of trajectories. We introduce the following simplified procedure which follows four steps:

- We first calculate the transmission coefficients at three selected points (1,2,3) at which the main body-fixed axes (x,y,z) respectively cross the nuclear surface (see Fig. A1). The coordinate system is chosen such that the rotation axis coincides with the x-axis and the z-axis is the symmetry axis.

For all possible values of the angular momentum of the emitted particle

$$\ell = |\vec{r}_i \times \vec{p}_i| = r_i p_{i\parallel} , \quad (A1)$$

where $p_{i\parallel}$ is the component of the vector \vec{p} parallel to the nuclear surface, and for each of the points (i=1,2,3) w is calculated using the Hill-Wheeler WKB expression [23]

$$w_\nu(e, \ell, \ell_x; i) = \left(1 + \exp\left[-\frac{2\pi(E_B - e)}{\hbar\omega_i}\right] \right)^{-1} . \quad (A2)$$

Here e is the single-particle energy and the barrier height E_B corresponds to the maximum of the potential V_{tot} in the direction $r_{i\perp}$ perpendicular to the surface. The potential in which the particle moves is given by:

$$V_{tot} = V_{nucl} + V_{cent} + V_{Coul} - \omega\ell_x \quad (A3)$$

i.e. by the sum of nuclear [1], centrifugal and Coulomb (in the case of charged particles) single-particle potentials. The quantity $\hbar\omega_i$ appearing in (A2) is given by

$$\hbar\omega_i = \hbar \sqrt{\frac{d^2 V_{tot}(i)/dr_{i\perp}^2}{m_\nu}} . \quad (A4)$$

- Once $w_\nu(e, \ell, \ell_x; i)$ is fixed at the three points (i=1,2,3) one averages in a second step over all possible values of the x-component of ℓ which is the component along the rotation axis. Such a procedure seems to be reasonable once the angular momentum of the emitted particles is not measured experimentally.

Through this average procedure one obtains

$$\bar{w}_\nu(e, \ell; i) = \frac{\sum_{\ell_x=-\ell}^{\ell} w_\nu(e, \ell, \ell_x; i)}{2\ell + 1} , \quad i = 1, 2, 3 . \quad (A5)$$

- The transmission coefficients $\bar{w}_\nu(e, \ell; i)$ being determined at the three selected points ($i=1,2,3$) one carries out in a third step an interpolation which allows to calculate the transmission coefficients to any point (θ, φ) of the nuclear surface

$$\bar{w}_\nu(e, \ell; \theta, \varphi) = \sin^2 \theta \cdot (\bar{w}_1 \cos^2 \varphi + \bar{w}_2 \sin^2 \varphi) + \bar{w}_3 \cos^2 \theta . \quad (A6)$$

This interpolation of quadrupole type ensures that the transmission coefficient in the directions along the main axes are the same as those for emission in the opposite direction.

- Finally one averages the coefficients over the whole nuclear surface:

$$\bar{w}_\nu(e, \ell; \chi) = \frac{\int_S \bar{w}_\nu(e, \ell; \theta, \varphi) d\sigma}{\int_S d\sigma} . \quad (A7)$$

The procedure described above incorporates in an approximate way the effects of nuclear deformation and rotation on the transmission coefficients.

Table caption

1. Results of precission neutron, proton and alpha multiplicity model calculations for ^{160}Yb at excitation energies 251 MeV and 293 MeV compared with the experimental data taken from Ref. [9]. The theoretical results are averaged over all initial angular momenta with a weight proportional to the corresponding fission rates.

Figures captions

1. Emission widths for neutrons (n), protons (p) and alpha particles (α) emitted from the hot, rotating compound nucleus ^{160}Yb ($E^*=50$ MeV, $L=40\hbar$) as a function of the elongation.
2. The same as in Fig. 1 but for $E^*=150$ MeV.
3. The same as in Fig. 1 but for $E^*=250$ MeV.
4. Emission widths for neutrons emitted from ^{160}Yb at $E^*=150$ MeV and $L=0, 20, 40$ and $60\hbar$ as a function of the elongation.
5. The same as in Fig. 4 but for protons.
6. The same as in Fig. 4 but for alpha particles.
7. Emission widths for neutrons emitted from different isotopes of Gd and Yb at $E^*=150$ MeV and $L=40\hbar$ as a function of the elongation.
8. The same as in Fig. 7 but for protons.
9. The same as in Fig. 7 but for alpha particles.
10. Probabilities to emit a neutron with energy smaller than e_n from the fissioning nucleus ^{160}Yb for three deformations corresponding to the spherical shape, the top of the fission barrier and the scission point.
11. The same as in Fig. 10 but for protons.
12. The same as in Fig. 10 but for alpha particles.
13. Probability to emit a neutron with energy smaller than e_n for three excitation energies ($E^*=50, 150$ and 250 MeV) of the fissioning nucleus ^{160}Yb .
14. The same as in Fig. 13 but for protons.
15. The same as in Fig. 13 but for alpha particles.

16. Number of trajectories out of sample of 10.000 leading to fission as a function of time with particle emission turned off. The calculation is done for three different temperatures ($T=3, 4$ and 5 MeV) of the fissioning nucleus ^{160}Yb . The heights of the corresponding fission barriers (U_B) are indicated in the figure.
17. Multiplicity of the prefission neutrons (n), protons (p) and alpha particles (α) as a function of time.
18. Ratio between the number of trajectories leading to fission and the total number of trajectories as a function of time for ^{160}Yb . The emission of the light particles is taken into account.
19. Energy spectra of neutrons (n), protons (p) and alpha particles emitted in coincidence with the fission events (solid lines). The dashed lines correspond to the spectra of the particles emitted from nuclei which end up as evaporation residua.
20. Yield of neutron emission P_n as a function of the deformation of the fissioning nucleus ^{160}Yb with initial excitation energy $E^*=293$ MeV and initial angular momentum $L=52\hbar$. The solid line corresponds to the trajectories which lead to fission while the dashed line to those leading to evaporation residua. The dotted line describes the distribution when the emission of protons and alphas is turned off.
21. The same as in Fig. 20 but for $L=45\hbar$.
22. Multiplicity of prefission neutrons (n), protons (p) and alpha particles (α) as a function of angular momentum of the compound nucleus ^{160}Yb with the initial excitation energy $E^*=251$ MeV.
23. The same as in Fig. 22 but for the excitation energy $E^*=293$ MeV.
24. Ratio between the number of trajectories leading to fission and the total number of trajectories as a function of the initial angular momentum for two different excitation energies $E^*=251$ MeV and 293 MeV.
25. Fission barrier heights as a function of the initial angular momentum for two different excitation energies $E^*=251$ MeV and 293 MeV.
26. Multiplicities of precission neutrons (n), protons (p) and alpha particles (α) as a function of the strength of the friction force.

Table 1

	$E^*=251$ MeV		$E^*=293$ MeV	
ν	model	exp.	model	exp.
n	5.98	6.10 ± 1.5	7.80	8.50 ± 1.6
p	0.94	0.51 ± 0.07	1.19	0.70 ± 0.08
α	0.58	0.48 ± 0.07	0.66	0.75 ± 0.08

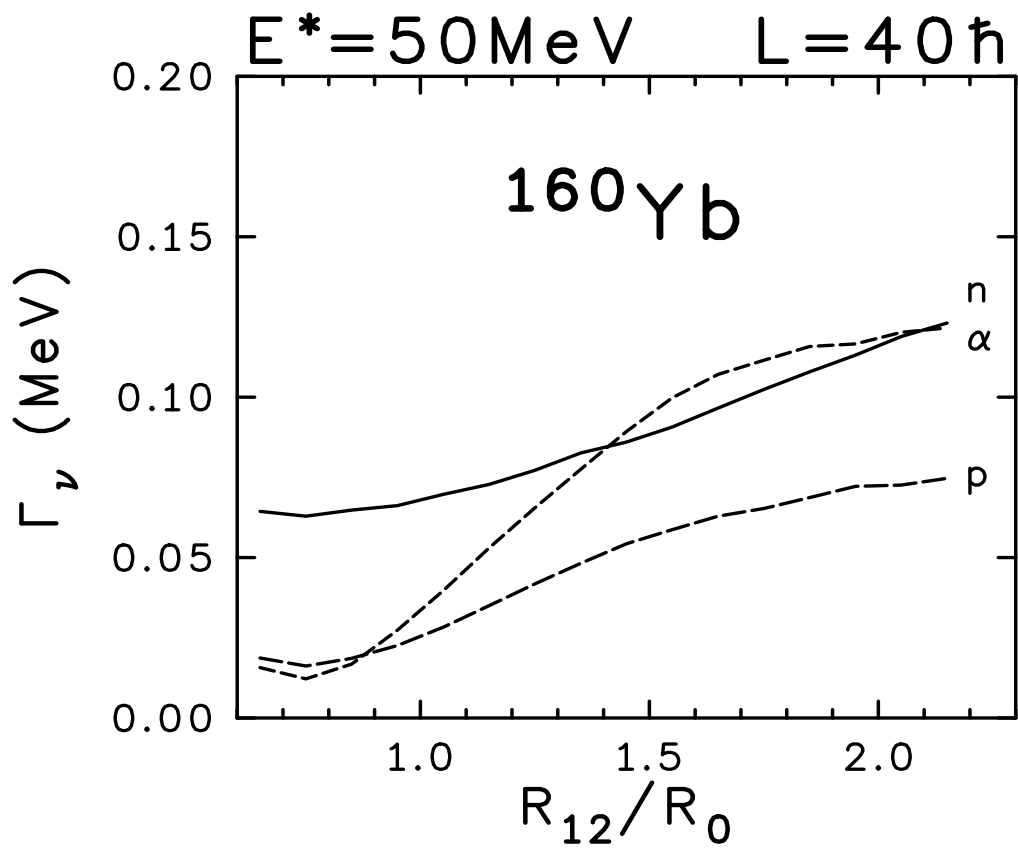


Figure 1

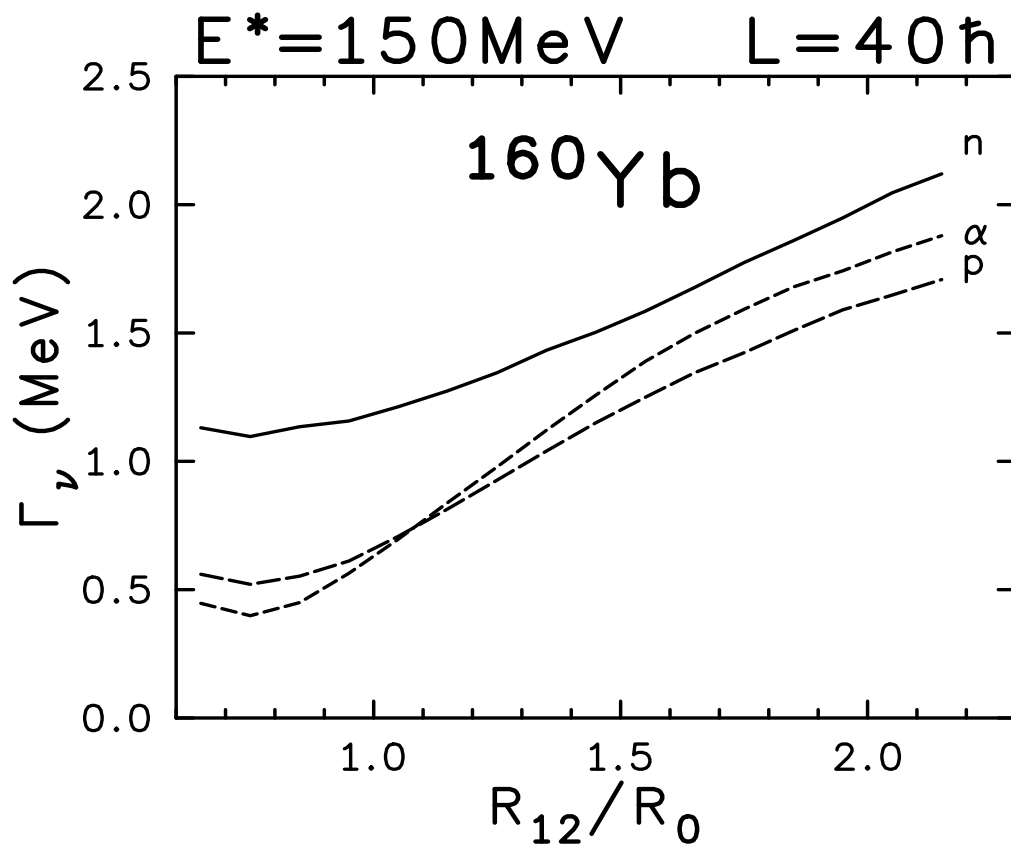


Figure 2

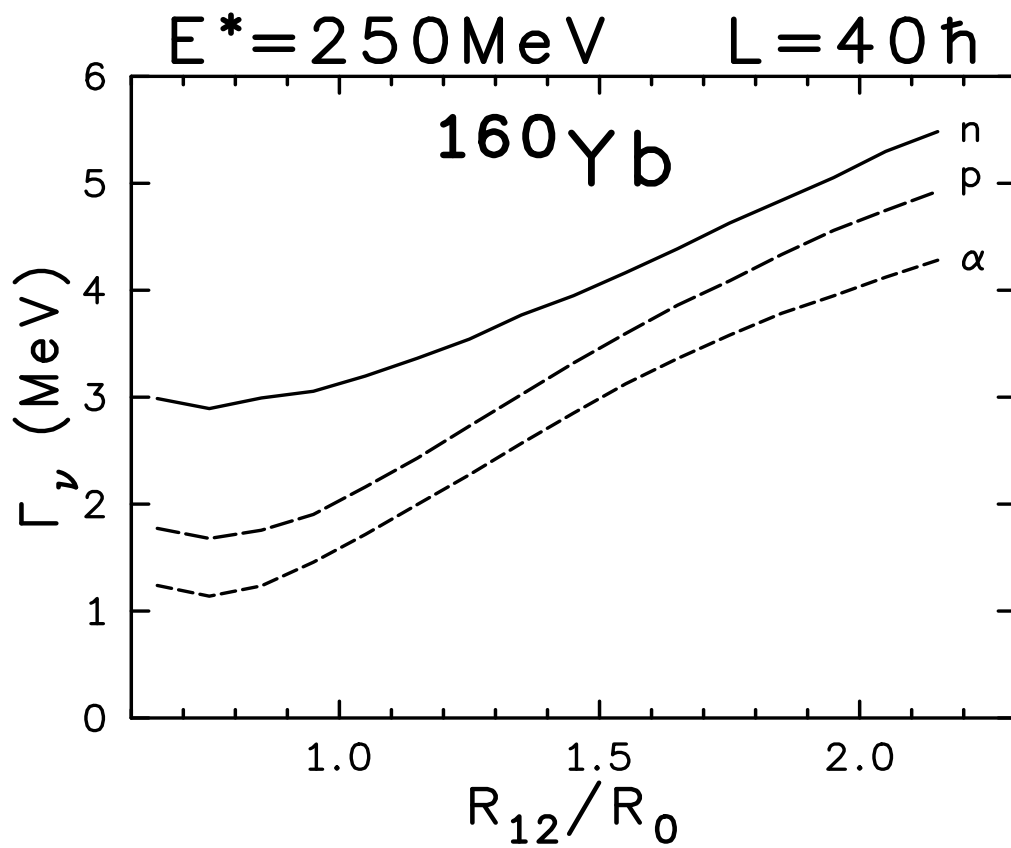


Figure 3

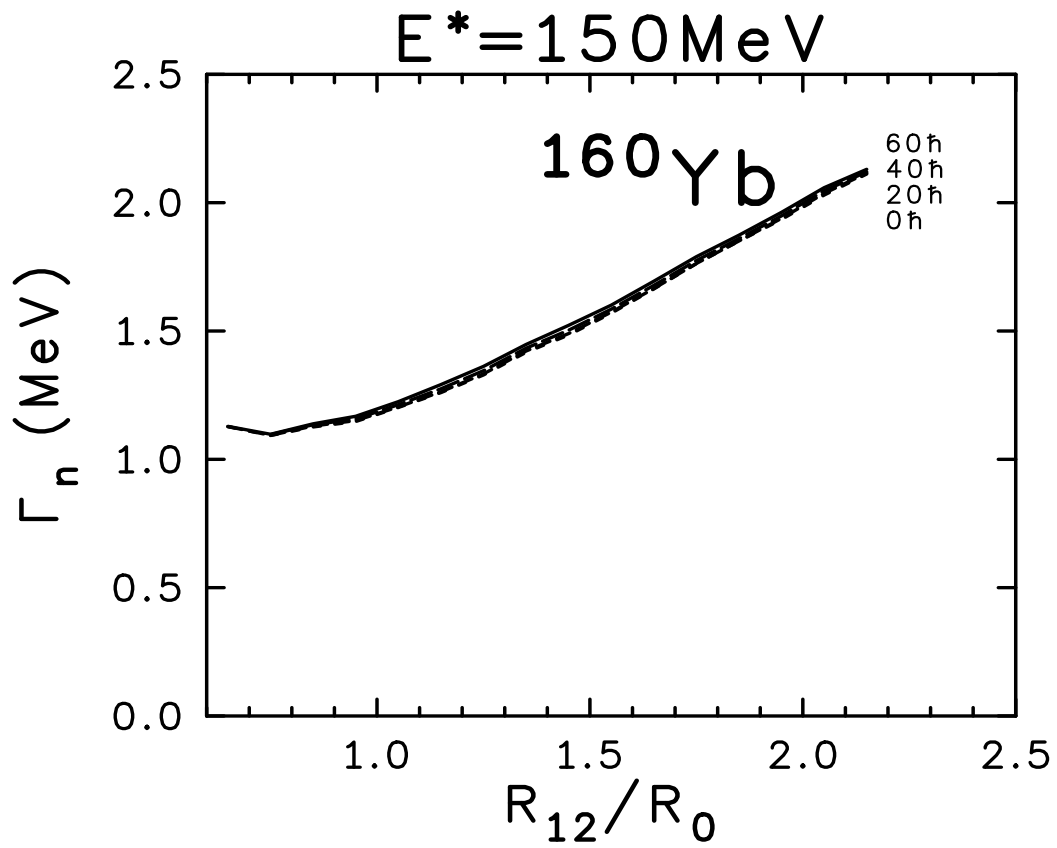


Figure 4

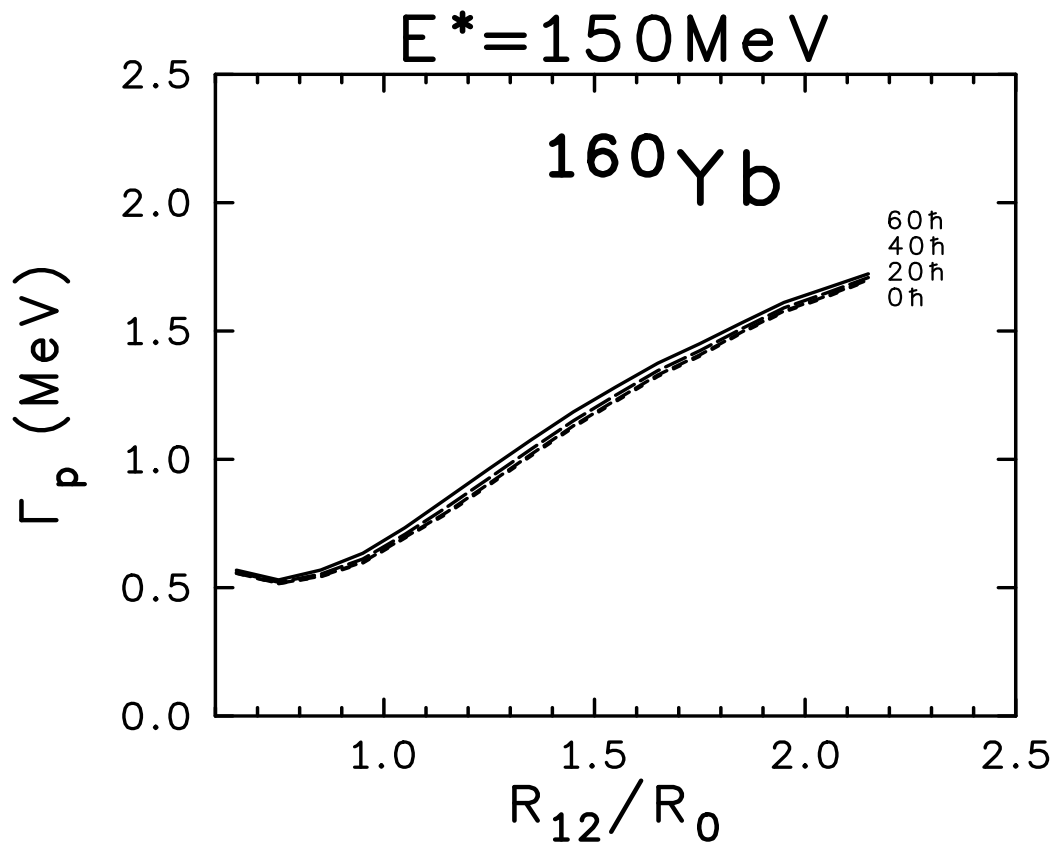


Figure 5

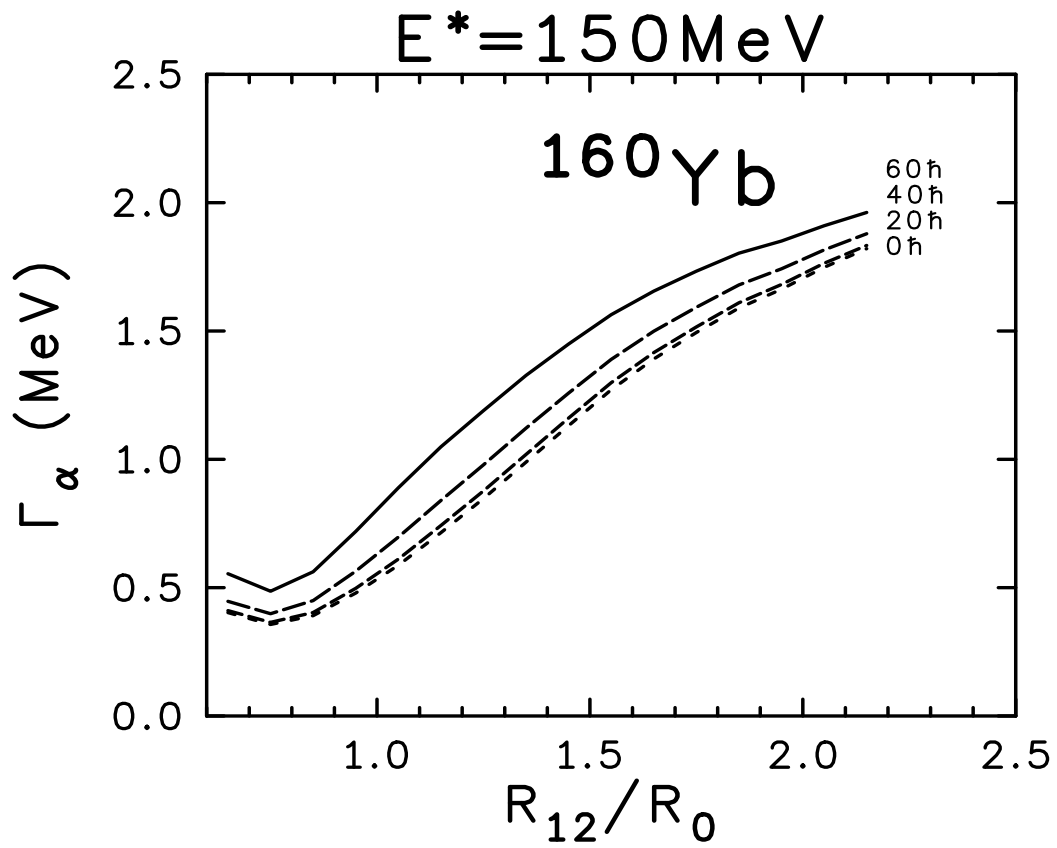


Figure 6

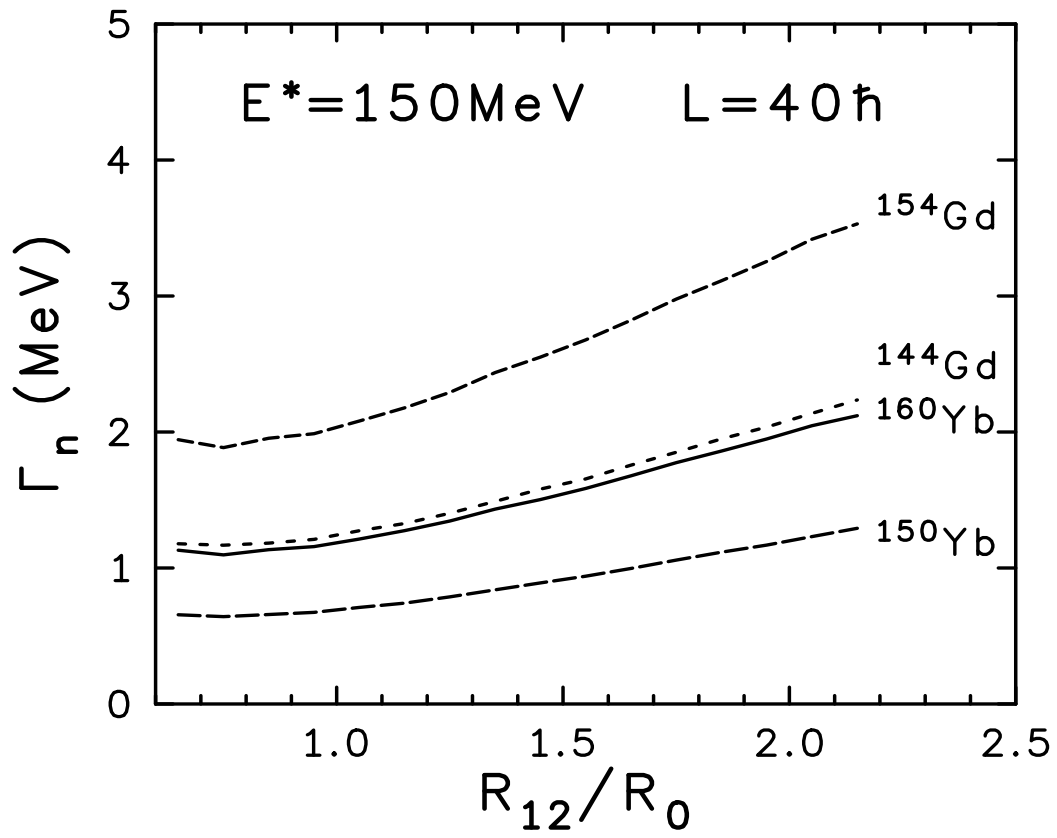


Figure 7

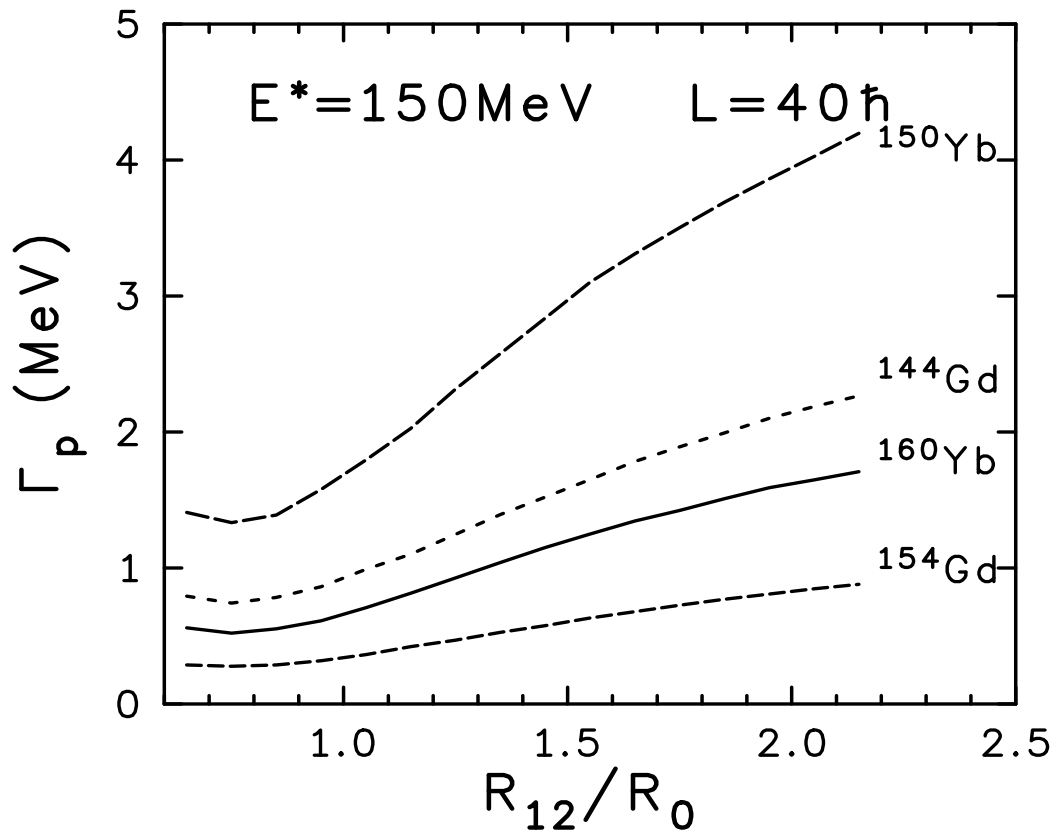


Figure 8

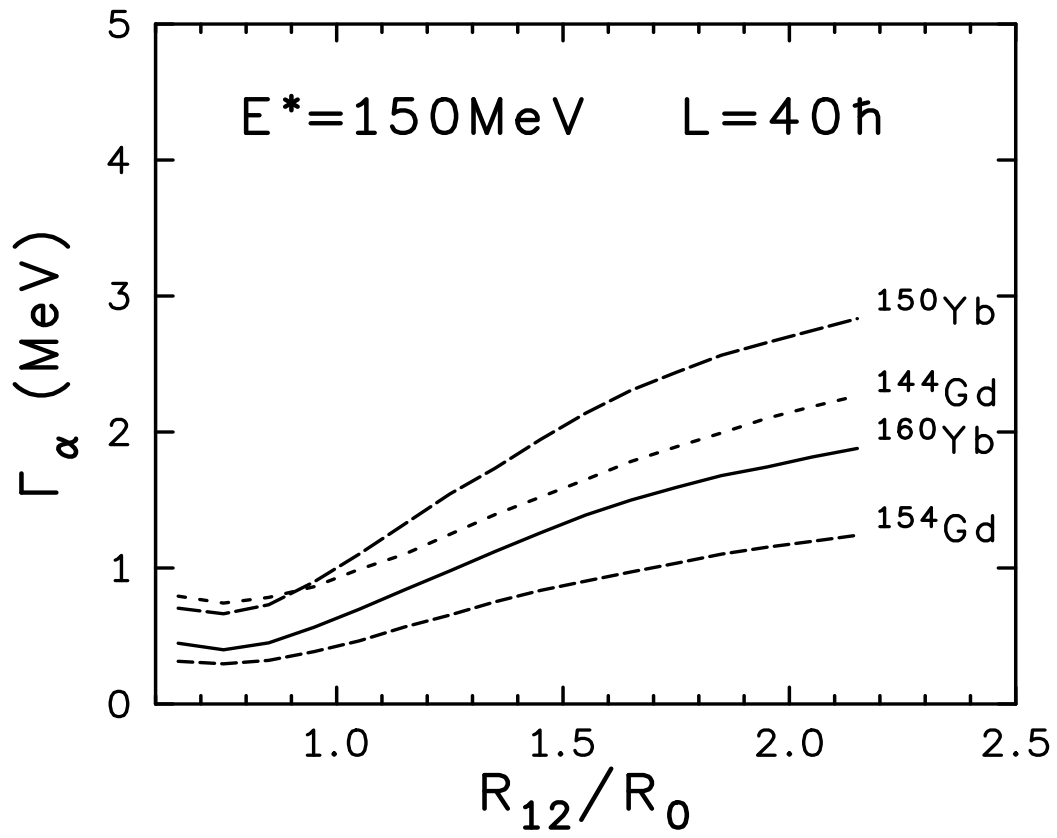


Figure 9

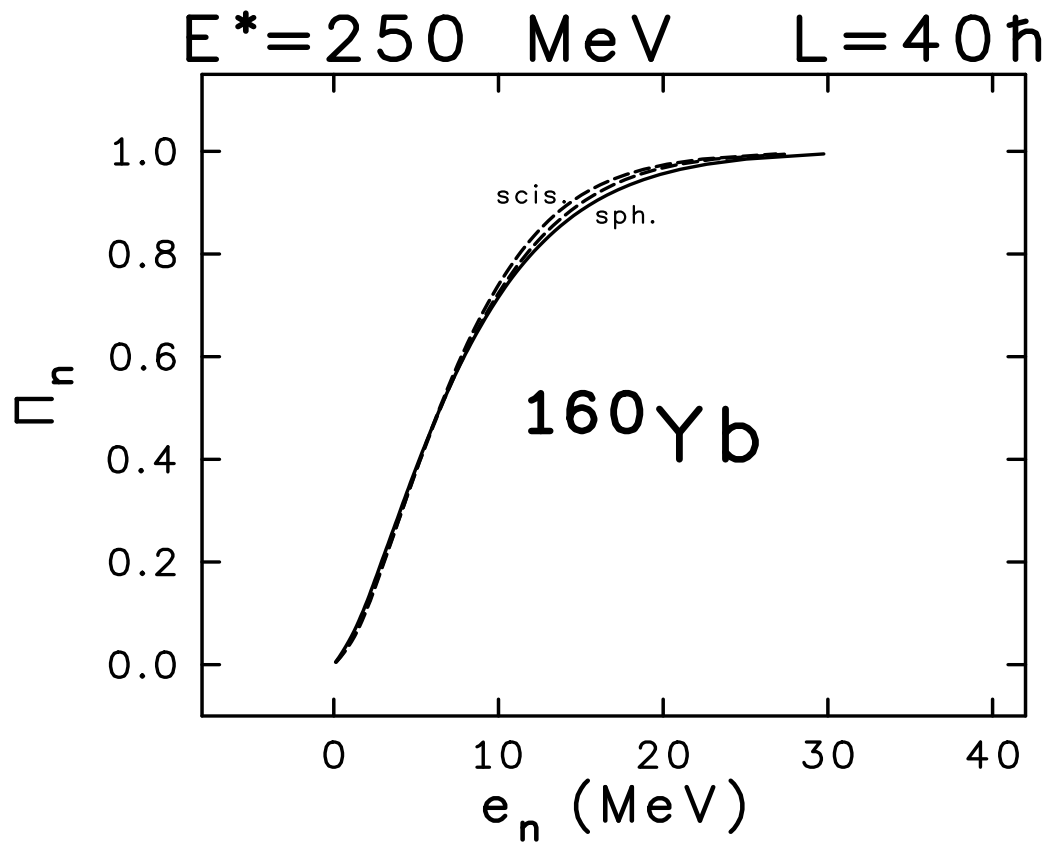


Figure 10

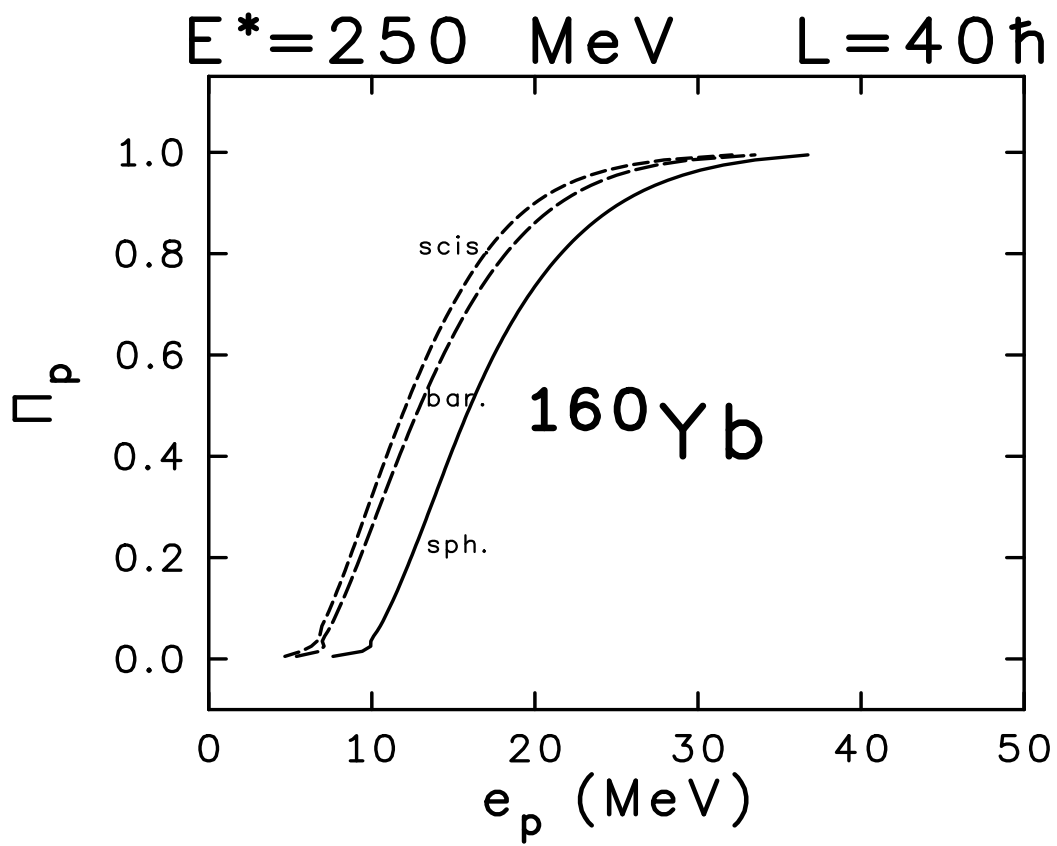


Figure 11

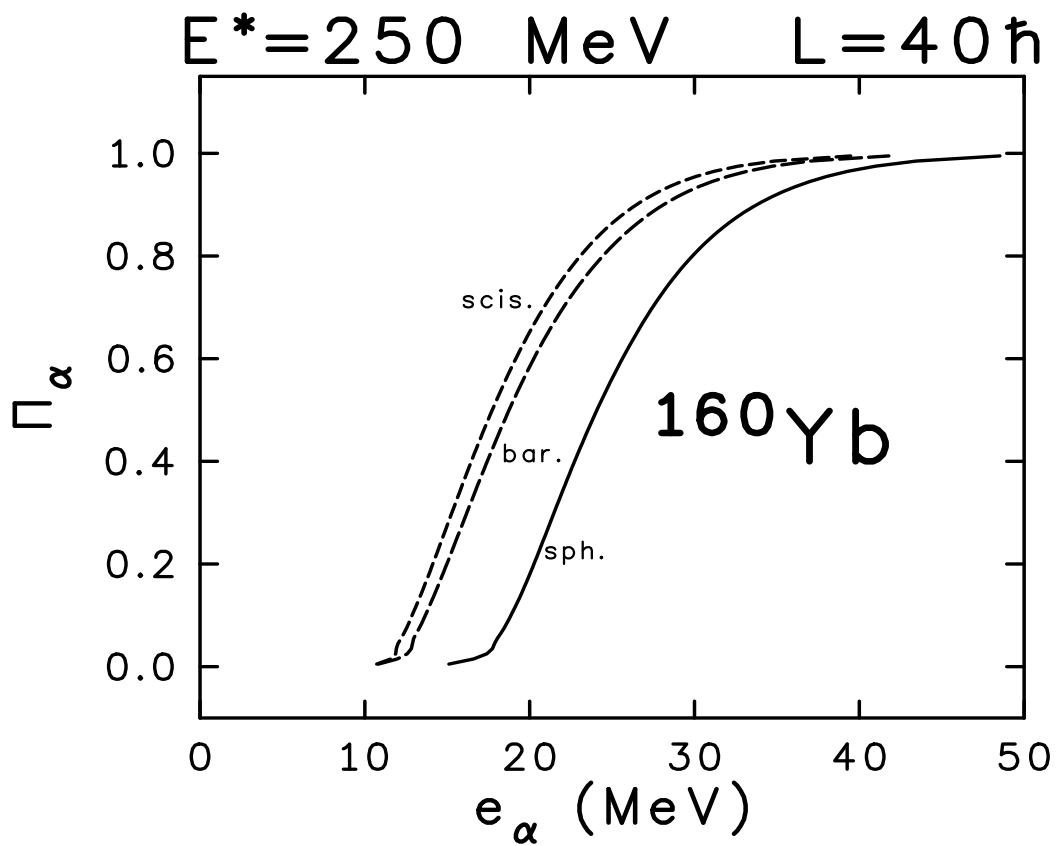


Figure 12

Saddle point, $L=40\hbar$

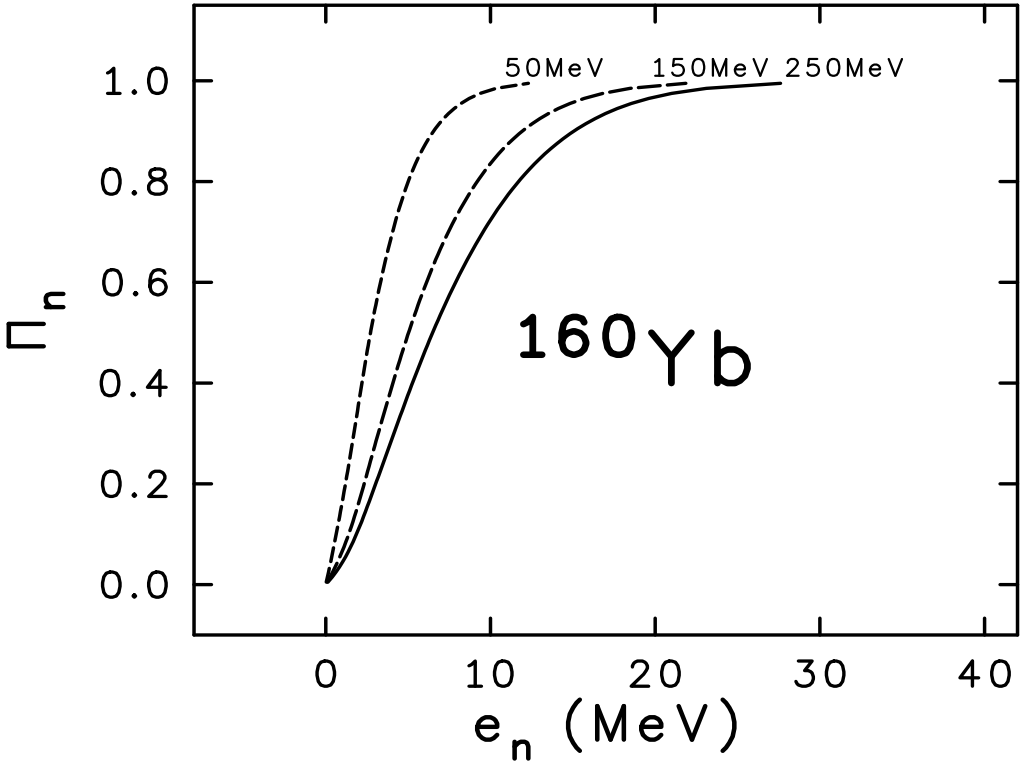


Figure 13

Saddle point, $L=40\hbar$

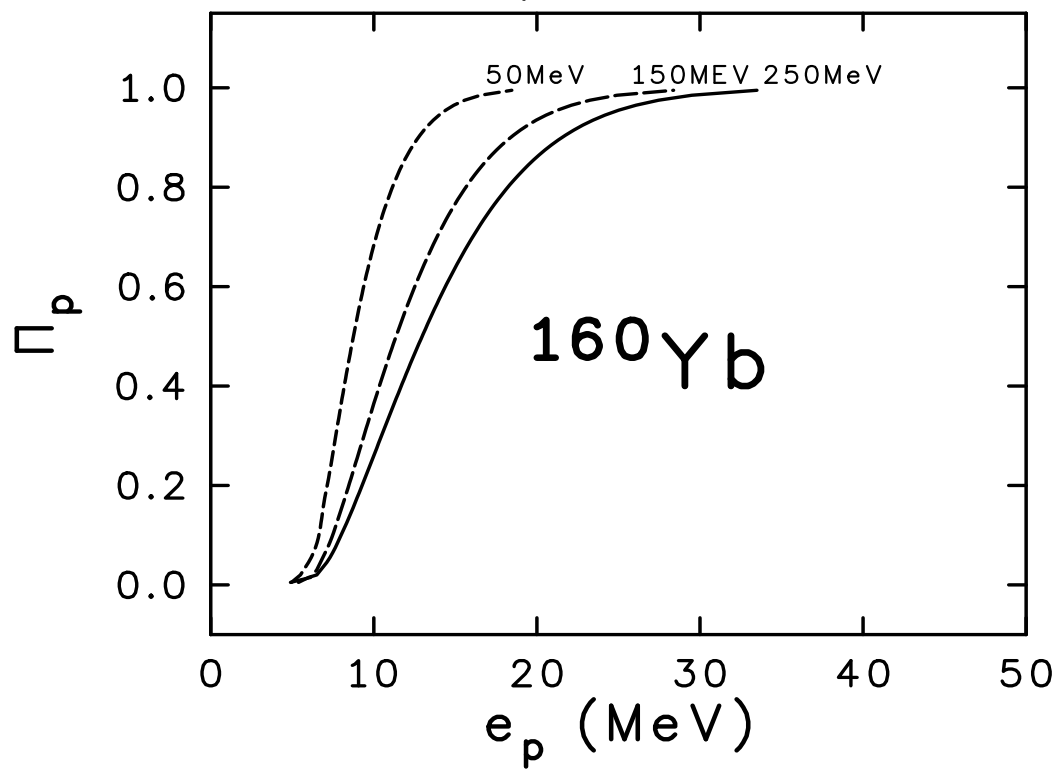


Figure 14

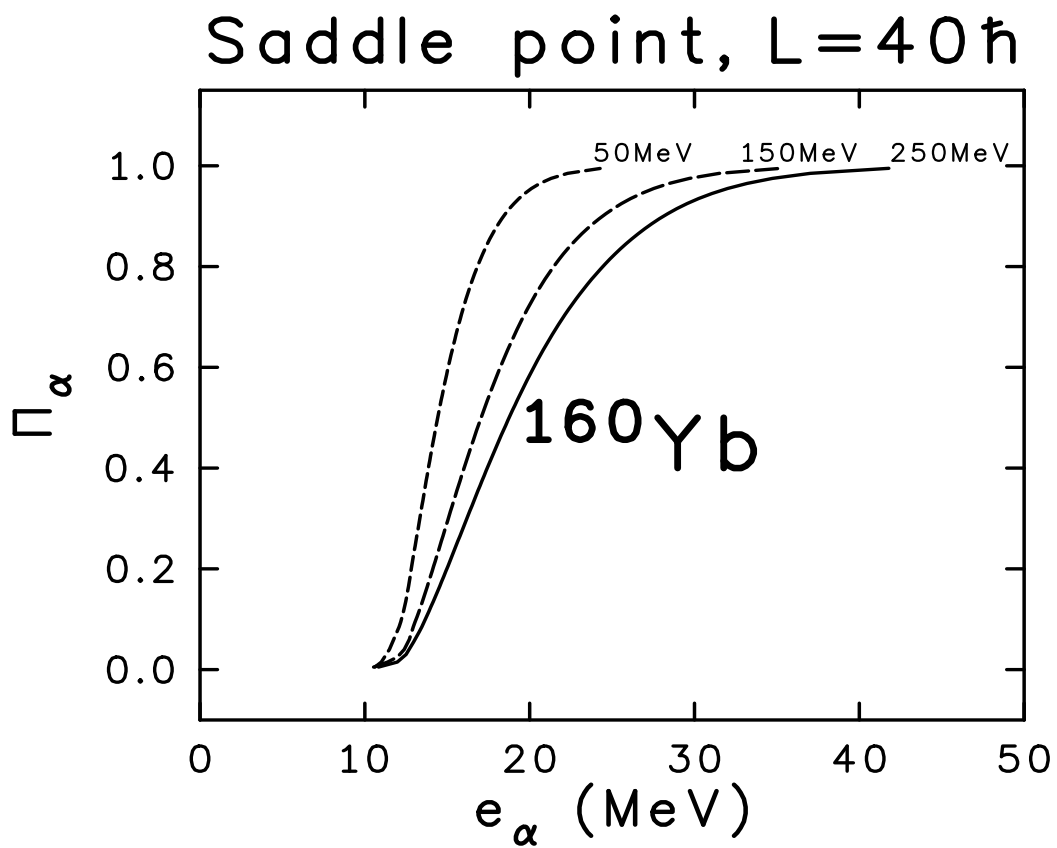


Figure 15

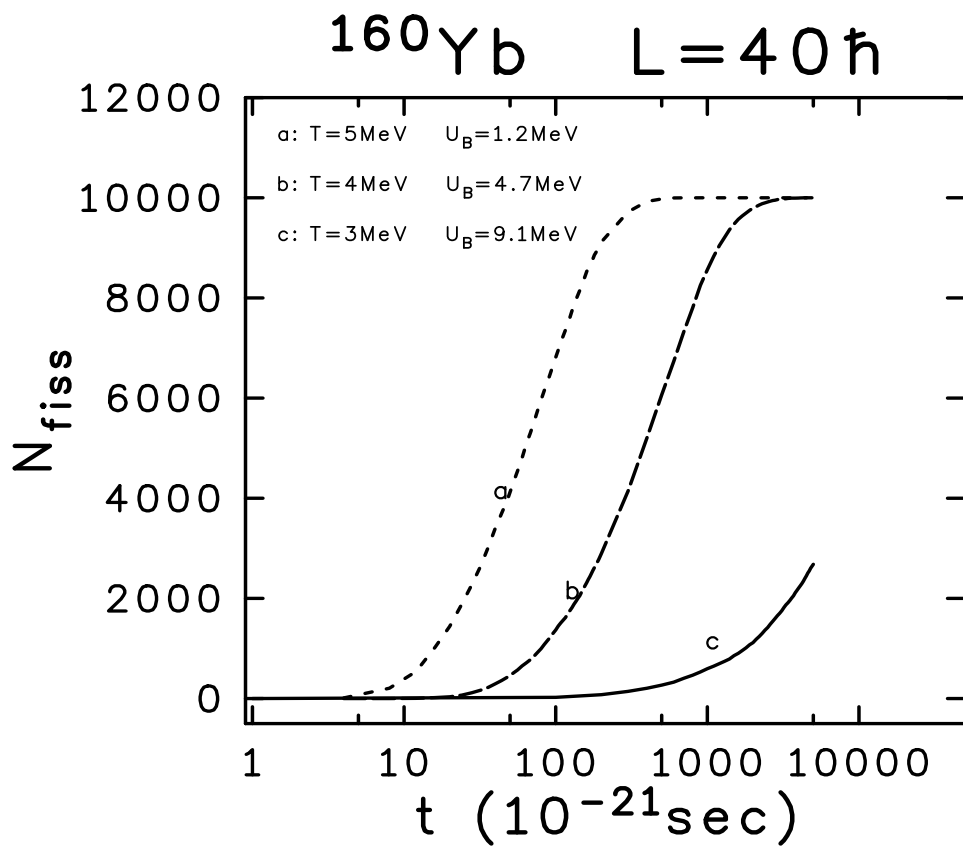


Figure 16

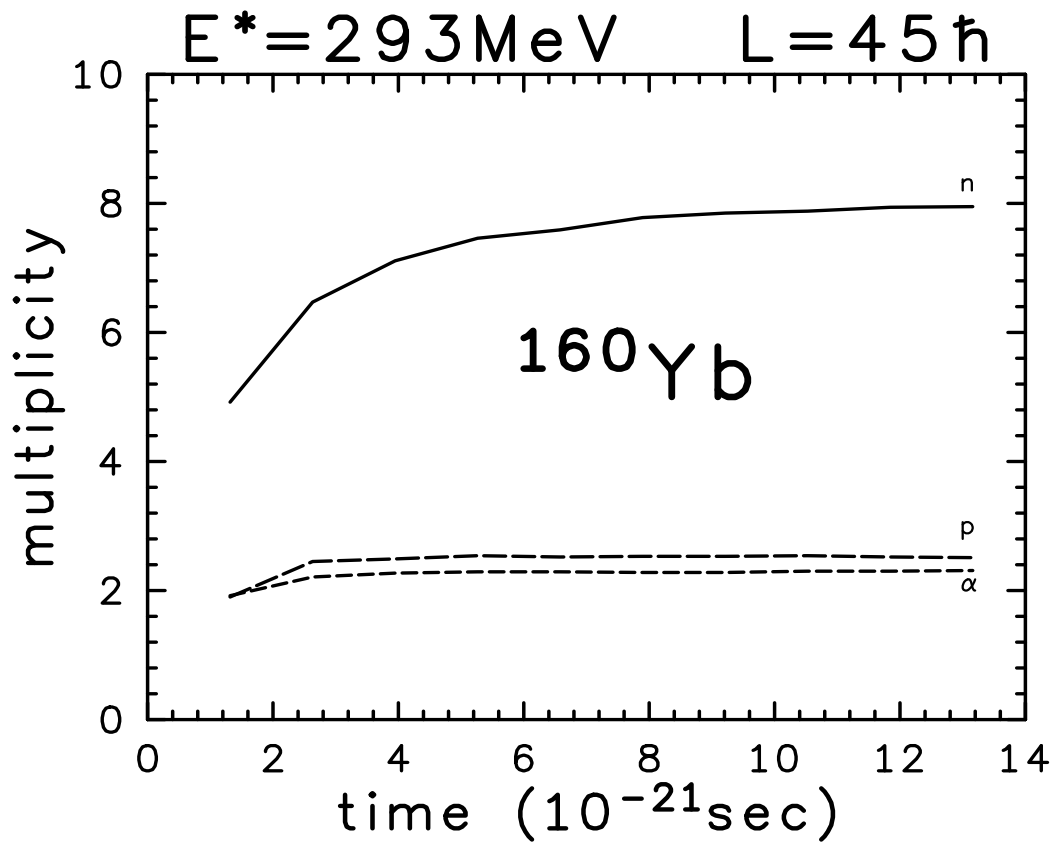


Figure 17

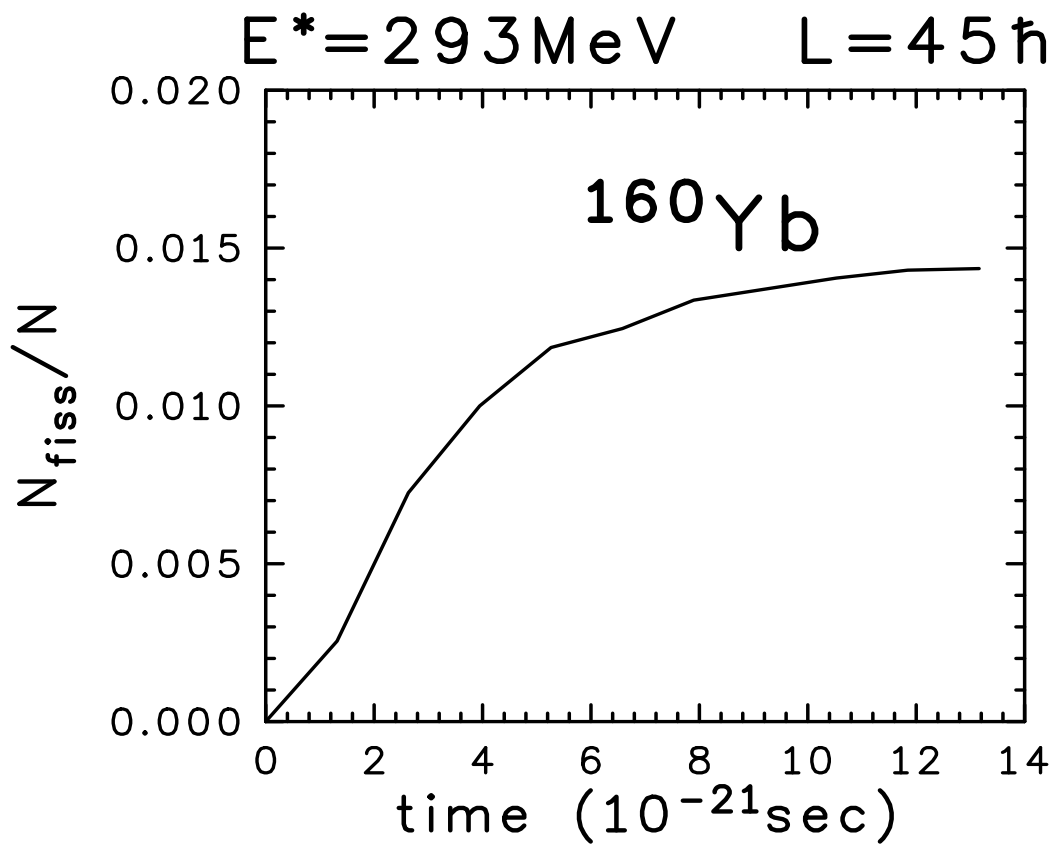


Figure 18

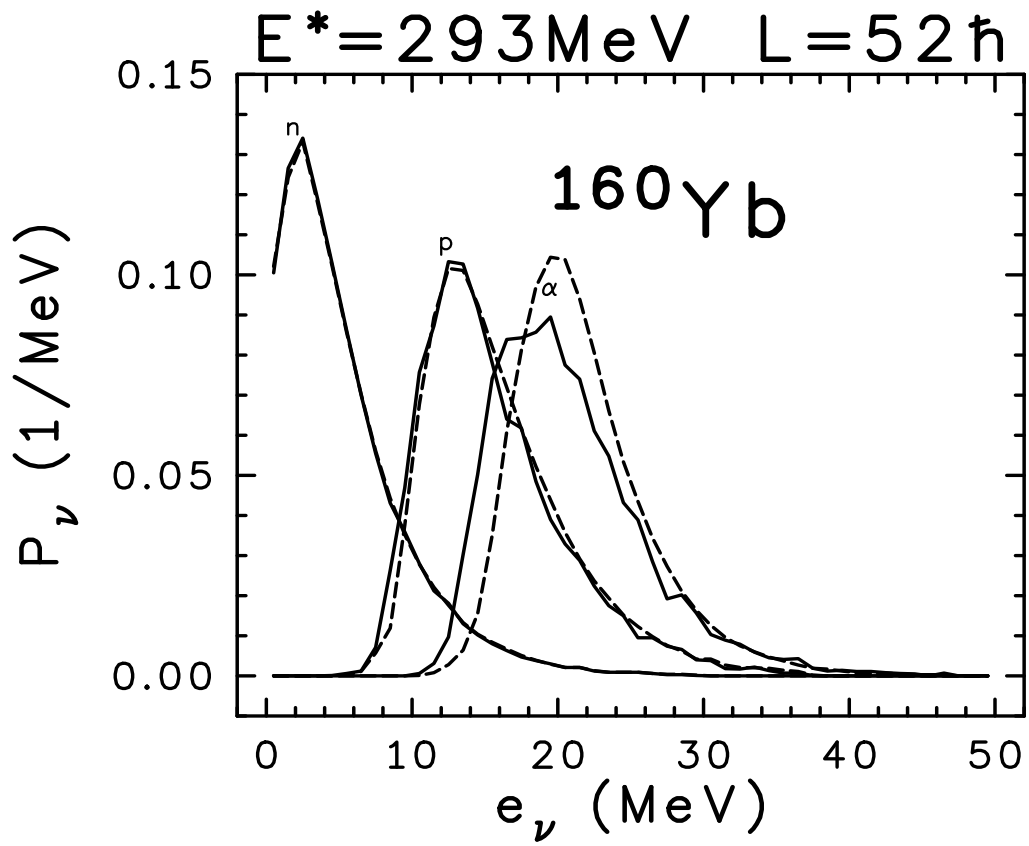


Figure 19

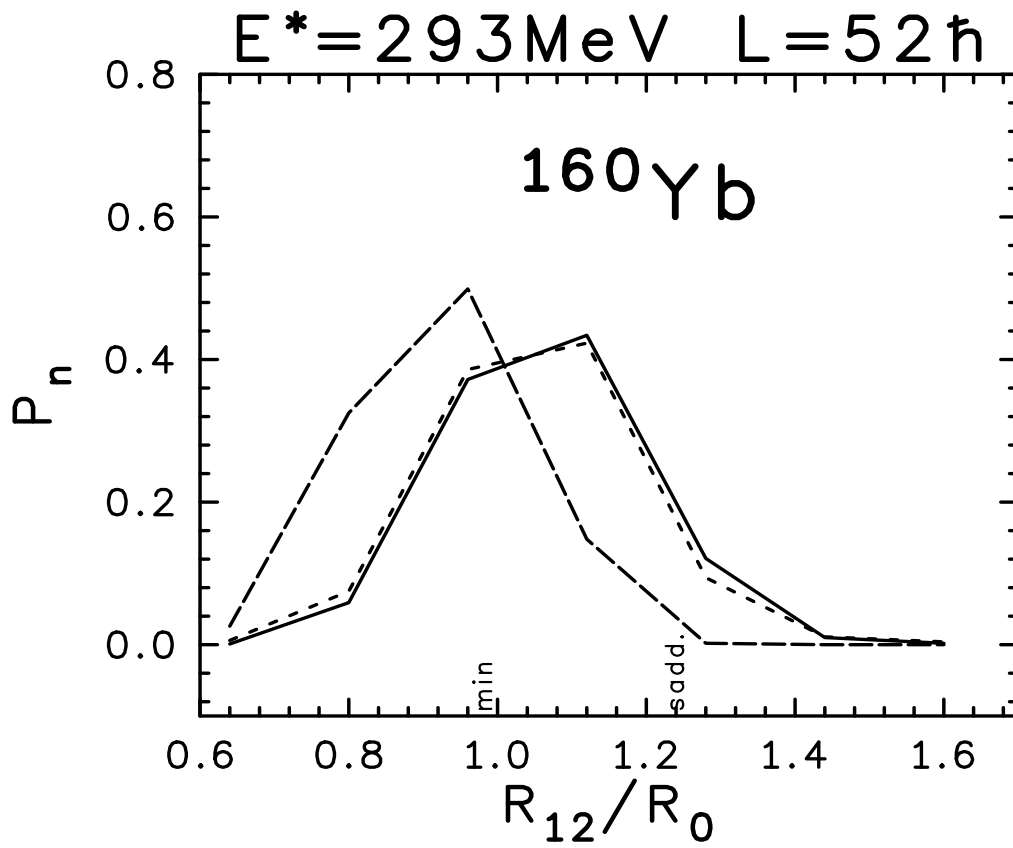


Figure 20

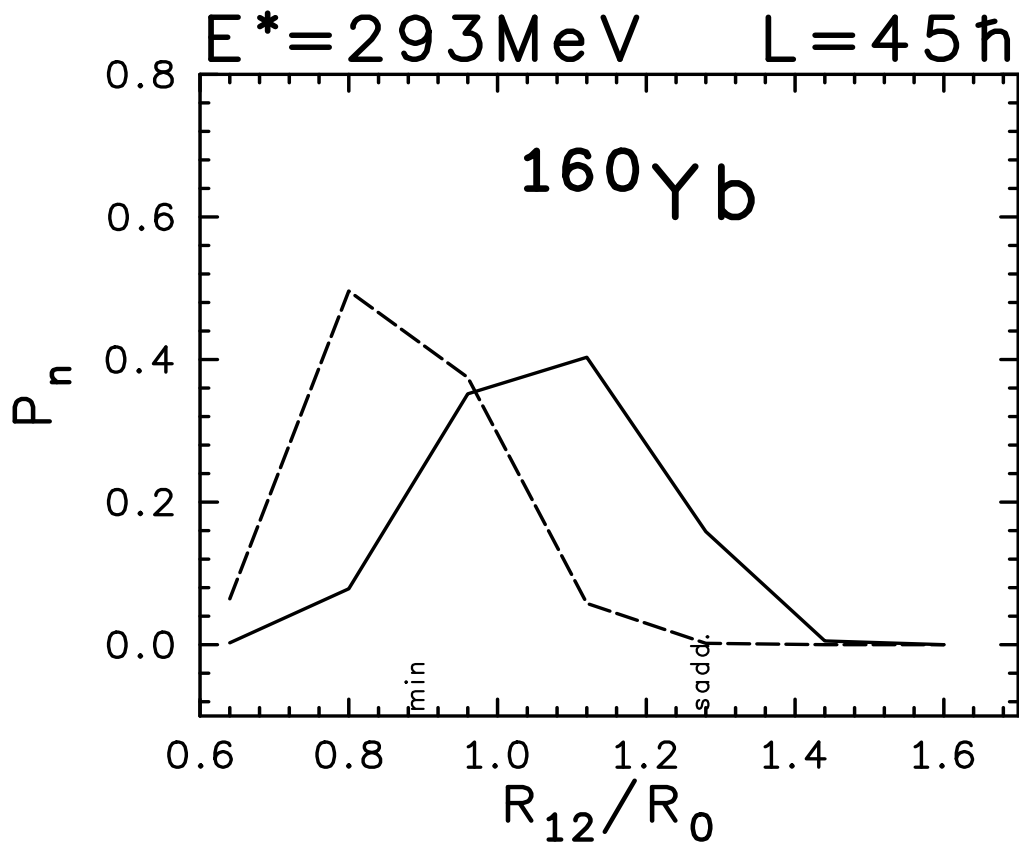


Figure 21

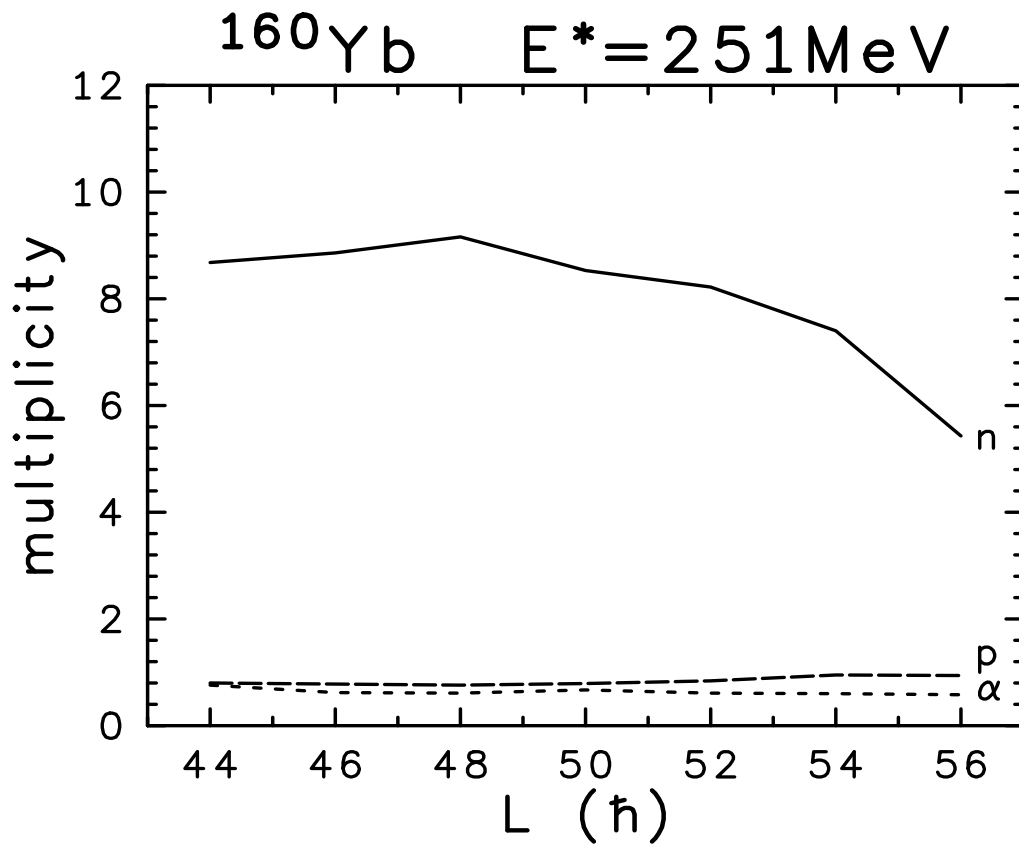


Figure 22

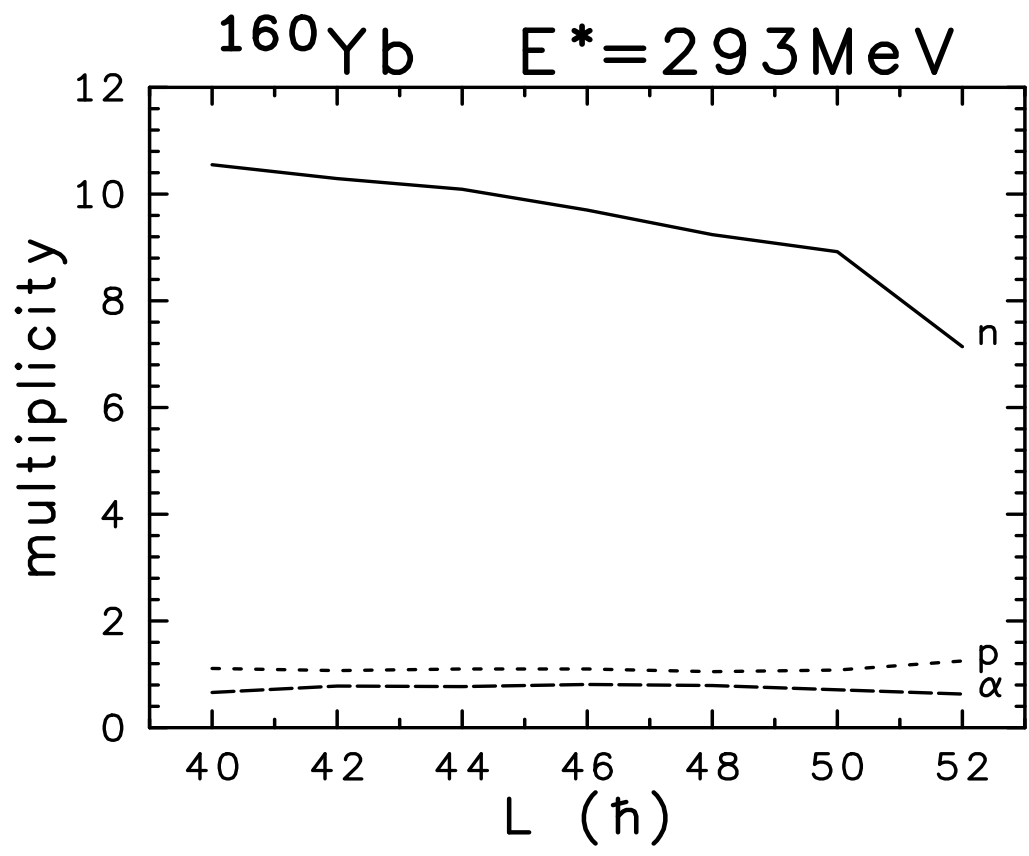


Figure 23

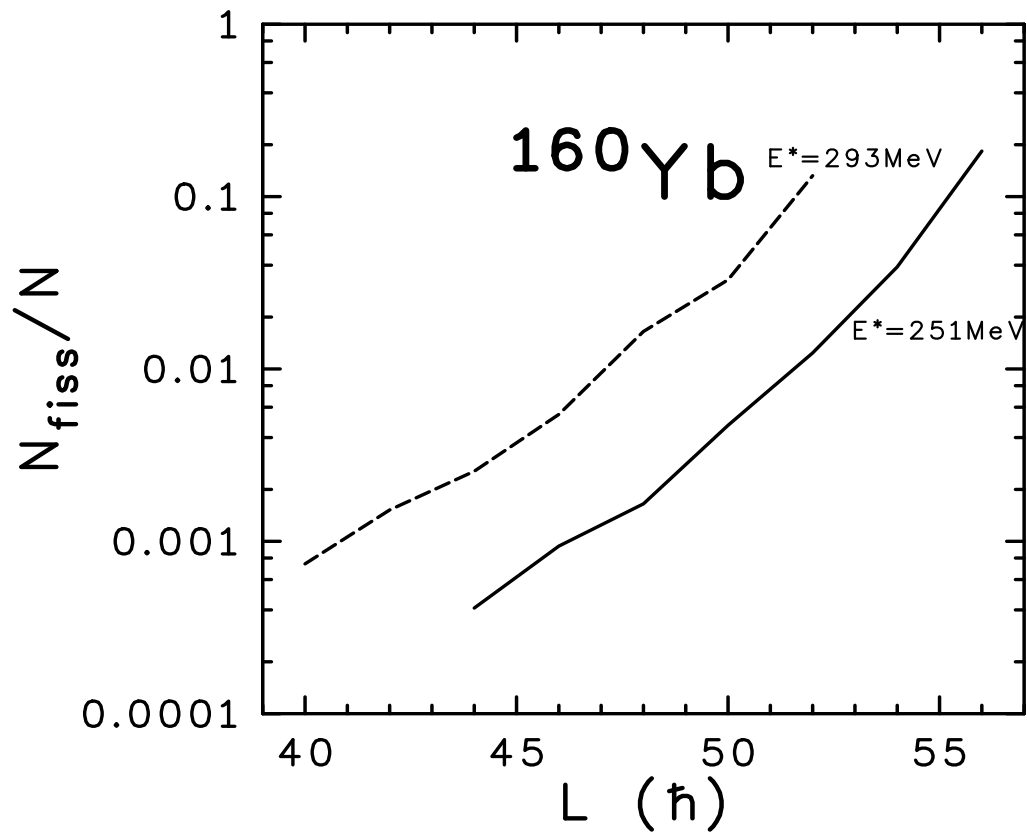


Figure 24

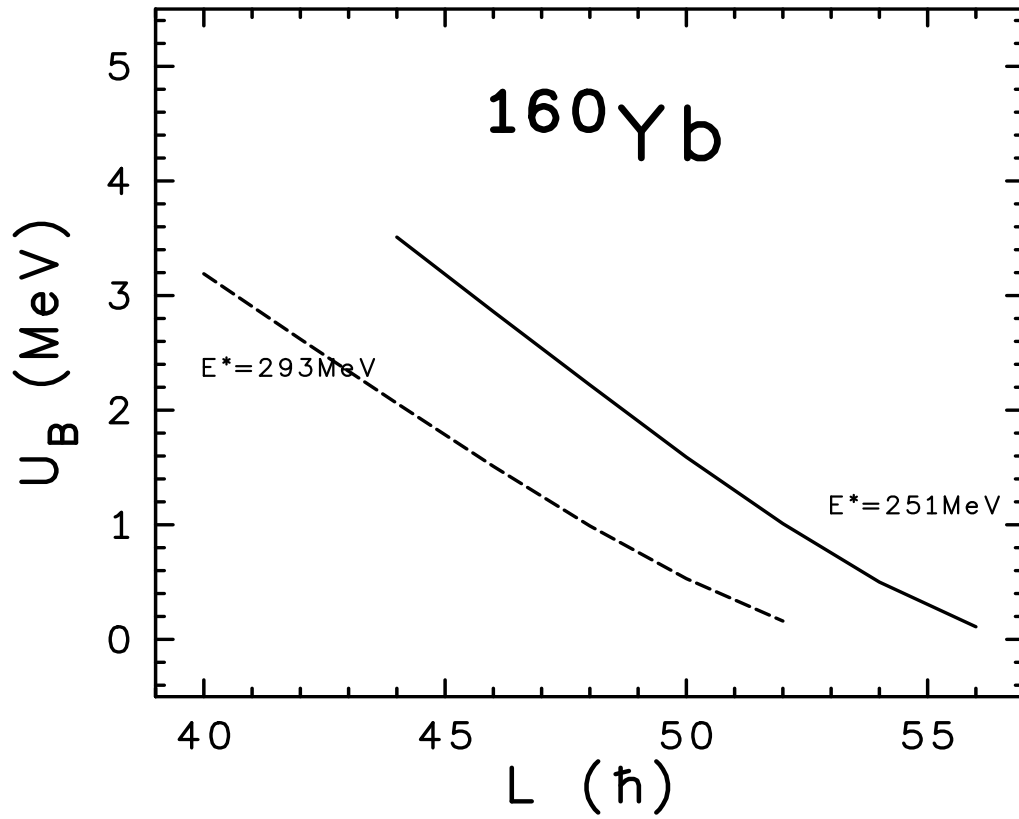


Figure 25

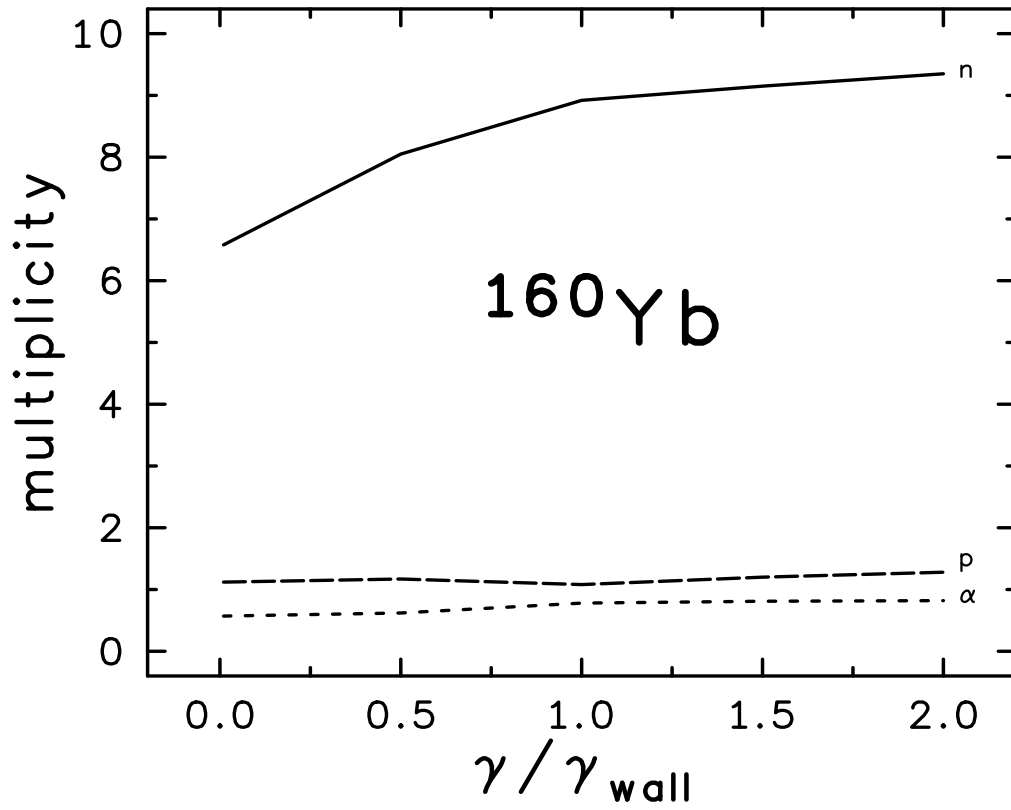


Figure 26